Faculdade de Engenharia da Universidade do Porto

A Wearable System for Remote Cardiorespiratory Fitness Monitoring

Marisa Alexandra Pinto Alves

FINAL VERSION

Dissertation Master in Biomedical Engineering

Supervisor: José Machado da Silva

September 2019

Resumo

Apesar dos diversos estudos desenvolvidos nos últimos para a melhoria do seu tratamento, as doenças cardiovasculares continuam a ser uma das maiores causas de morte da sociedade atual. Entre estas doenças, destaca-se a insuficiência cardíaca, uma doença caracterizada pela incapacidade do músculo cardíaco de bombear sangue para todo o corpo. Ainda relativamente a esta doença, estudos preveem que se verifique um aumento de cerca de 33% do número de pacientes diagnosticados com esta doença em Portugal até 2035, o que vem realçar a importância do desenvolvimento de soluções que não só potenciem o seu tratamento, como também minimizem os custos necessários para tal.

Atualmente, o tratamento da insuficiência cardíaca passa pela utilização de fármacos numa primeira instância, seguida de uma fase em que o autocuidado dos pacientes é fulcral para se atingirem os melhores resultados possíveis. Este cuidado consigo próprio, quando deficiente, leva a uma hospitalização recorrente, ou então mesmo a complicações graves por incompreensão dos sintomas. Tudo isto, associado ainda ao facto de que muitos dos pacientes que padecem desta doença apresentam também incapacidades motoras, leva a que o desenvolvimento de um sistema que auxilie a monitorização remota destes pacientes é algo deveras vantajoso, não só em termos de saúde, mas também económicos. Esta preocupação não é, assim, nova: existem já no mercado dispositivos que permitem a monitorização de pacientes com doenças cardiovasculares. No entanto, para uma monitorização o mais eficiente possível, seria necessária a implementação num mesmo dispositivo de sensores de diferentes grandezas, tais como bioimpedância elétrica, de pulsação, de oximetria, eletrocardiográficos e ainda químicos, que permitissem a determinação da concentração de NaCl no suor, o que ainda não existe.

O trabalho realizado nesta dissertação consistiu no desenvolvimento de um sistema de monitorização remota de pacientes com insuficiência cardíaca composto por um dispositivo de captura de sinais eletrocardiográfico, de oximetria e de pressão artéria, que comunica com uma aplicação de telemóvel que recebe e faz uma pré-análise dos dados capturados, e os envia para um servidor remoto onde são registados e disponibilizados para consulta por profissionais de saúde.

Abstract

Despite several studies in the past to improve its treatment, cardiovascular disease remains one of the leading causes of death in today's society. Among these diseases, heart failure, a condition characterised by the inability of the heart muscle to pump blood throughout the body, stands out. Still, regarding this disease, studies predict that there will be an increase of about 33% in the number of patients diagnosed with heart failure in Portugal by 2035, which highlights the importance of developing solutions that not only potentiate their treatment but also minimise the costs required by this condition.

Currently, treatment for heart failure involves the use of drugs in the first instance, followed by a phase in which patient self-care is central to achieving the best possible results. This self-care, when deficient, leads to recurrent hospitalisation or even severe complications due to the misunderstanding of symptoms. All this coupled with the fact that many of the patients suffering from this disease still have motor disabilities, the development of a system to assist this monitoring is very advantageous, not only in terms of health but also for the economic side. This concern is therefore not new: there are already devices on the market that include implantable or non-implantable systems aimed at determining some important measure for monitoring patients with cardiovascular disease. However, for the most efficient monitoring possible, it would be necessary to implement electrical bioimpedance, oximetry, electrocardiographic and even chemical sensors that would allow the determination of NaCl concentration in sweat, which have not yet been implemented.

That said, the work developed during this dissertation consists of the development of a remote monitoring system for patients with heart failure. This system consists in a device for the electrocardiographic, oximetry and artery pressure signal capture, which communicates with a mobile phone application that receives and pre-analyses the captured data and sends them to a remote server where they are recorded and made available for consultation by healthcare professionals

Acknowledgements

Para começar, e como não podia deixar de ser, deixo o meu maior agradecimento ao meu orientador, o Professor José Machado da Silva, por me ter feito sair da minha área de conforto e enrredar por um caminho que não seria o mais lógico, mas que me motivou do inicio ao fim e me fez sentir que valeu a pena ter mudado de projeto numa fase em que normalmente não mudaria.

Tenho também que agradecer a todos os meus amigos, mas acima de tudo a todos aqueles que constituem o "congresso MEBiano" e que contribuíram para que estes dois anos fossem ainda mais incríveis. Às tardes de estudo, aos jantares, aos acampamentos e a todos os momentos que me fizeram aguentar as alturas menos boas que foram acontecendo. Um especial obrigada à Raquel, à Bia e à Cat pelos jantares extra seguidos de noites de estudo e que tão bem sabiam. E Ju, não tenho palavras para te agradecer. Os almoços até às quatro da tarde, as conversas intermináveis, as mensagens de motivação diária que nunca faltavam nesta fase final… simplesmente obrigada.

À minha família, que apesar da distância e de nem sempre perceberem o que realmente estava a fazer, estiveram sempre presentes. Mãe e pai, consegui. À minha irmã, obrigada pelas conversas, pela paciência, pelas chamadas, por simplesmente estares sempre lá para mim. Sem ti, a vida não tinha nem metade da piada.

Por fim, e talvez porque seja aquele que mais teve de lidar com as minhas fases más em todo este processo, ao Zé Diogo. Obrigada pela ajuda, pela companhia, mas essencialmente obrigada pelos raspanetes que me faziam sair dos estados "menos bons" e voltar ao trabalho. Foste indispensável em todo este processo. E sim, sei que vou ter de te aturar de mau humor uma eternidade para compensar tudo o que aturaste.

Contents

List of Figures

List of Tables

Abbreviations

AC	Alternating Current
BLE	Bluetooth Low Energy
BP	Blood Pressure
bpm	Beats Per Minute
BV	Blood Volume
Cm	Cell Membranes
CO	Cardiac Output
DC	Direct Current
DIA	Diastolic
ECG	Electrocardiogram
ECG2C	Ecg 2 Click
EDA	Electro Dermal Activity
EMG	Electromyography
FAV	Fluid Accumulation Vest
FDA	Food and Drug Administration
FPCB	Flexible Wireless Printed Circuit Board
Hb	Haemoglobin
HbO2	Oxyhemoglobin
HF	Heart Failure
HP	Hypertension
HR	Heart Rate

HR4C	Heart Rate 4 Click
I2C	Inter-Integrated Circuit
ICG	Impedance Cardiography
IR	Infrared
LA	Left Arm
LED	Light-Emitting Diode
LL	Left Leg
LV	Left Ventricular
LVH	Left Ventricular Hypertrophy
MI	Myocardial Infarction
O2	Oxygen
SpO_2	Oxygen Saturation
P1	Shorter Period
P2	Pulse Period
PET	Polyethene Terephthalate
PPG	Photoplethysmography
PTT	Pulse Transit Time
PWV	Pulse Wave Velocity
R	Red
RA	Right Arm
Re	Extracellularly
Ros	Ratio of Ratios
SCL	Serial Clock
SDA	Serial Data
SPI	Serial Peripheral Interface
STT	Lope Transit Time
SYS	Systolic
TEB	Transthoracic Electric Bioimpedance

Chapter 1

Introduction

The initial chapter presents a brief description of this dissertation, including a resume of the subject under study, as well as the primary goal of the project and the structure of this document.

1.1 | Context and Motivation

Heart Failure (HF) is a cardiovascular disease that remains one of the most common, costly, disabling, and deadly diseases, affecting more than 25 million people worldwide [1]. Among the available treatment phases, self-care is one of the fundamental processes for the best recovery and prevention of chronic HF. This self-care implies that patients monitoring various symptoms, make proper use of medication, exercise and are able to manage symptoms, make behavioural changes or request assistance when needed [2]. However, and mainly due to the fact that many of these patients have cognitive dysfunction, the development of a system that enables active remote follow-up by the physician is crucial, and a way to reduce mortality and improve quality of life. To support the importance of this system, the follow-up of HF patients, even when accomplishing with medical home visits, has been shown to be cost-effective, being associated with a lower readmission rate and even mortality [3].

The use of technologies for remote patient monitoring, telemedicine, is already widely used in heart disease cases. Its use has two main objectives: to improve and individualise each treatment, as well as reduce the costs associated with the disease [4]. Concerning patients with HF, this technology is mainly applied using implantable devices, where information can be

taken from devices in addition to their therapeutic function, for example from cardioverter – defibrillator, or deploying devices whose sole purpose is monitoring [5]. Despite the evolution associated with these systems, these devices are invasive, having several times risks associates to the implantation, which leads to the necessitate the development of a non-invasive alternative. For this purpose, several devices capable of capturing different biomedical signals in a non-invasive way have been reported; however, none provide the measurements necessary for effective monitoring of patients with FH.

1.2 | Objectives

Technological evolution is something that one should undoubtedly take advantage of to improve health care. Given the improvements that an efficient monitoring system can bring to the treatment of patients with HF, the overall objective of this project is to develop a system for remote and minimally invasive patient monitoring.

It is necessary having in account that abnormalities in HF exist essential due to a variety of underlying diseases and health problems, such as coronary heart disease, diabetes and high blood pressure (BP) [6]. More than that, the HF begins typically in the left side of the heart, responsible for receives oxygen-rich blood from the lungs and pumps it into the left ventricle, the heart's largest and strongest pump, which is responsible for supplying blood to the body. When the left ventricle fails, fluid can back up to the lungs, leading to Pulmonary Oedema. In turn, pressure from the excess fluid can damage the heart's right side as it works to pump blood into the lungs. When the right ventricle fails, blood gets accumulated near the tissues, causing various oedemas, evident by the swelling of the respective body part. Apart from fluid congestion – often emphasised by the term Congestive HF -, symptoms such as high heart rate (HR), coughing, shortness of breath and some cognition dysfunctions are also associated with the disease. These data should then be made accessible through a mobile application and stored in a cloud service, accessible by the responsible physician [7]. Having said that, the system should include many sensors that allow capturing different data, such as electrical bioimpedance, electrocardiographic (ECG) and oximetric and ionic data, the latter through the detection of NaCl in the skin.

To obtain a first preliminary demonstration prototype, the developed monitoring device comprises only ECG and oximetry sensors, being arterial pressure obtained from the oximeter Photoplethysmography (PPG) signal.

1.3 | Document Structure

This document is structured in five more independent chapters, followed by bibliographical references, besides this first one, in which is possible to find the context and motivation that led to the accomplishment of this work, as well as the objectives of the project and the

structure of the presented document. The summary of the contents for each chapter are represented bellow.

Chapter 2 presents a review of the basic concepts of HF, including the diagnosis and the currently available treatments. It is still shown a detailed description of the several biomedical parameters that are important to qualify considering the purpose of this project.

In chapter 3, it is present a description of the principles behind the sensors needed to implement for an effective monitorization. This chapter describes the operation of the several sensors necessary to obtain the quantities mentioned in the previous section as well as a brief review of the implantable and non-implantable existing sensors.

Regarding chapter 4, it describes the system architecture. This includes the choice of hardware used, as well as a brief description of the communications required to implement the various click boards used. It also describes the software used for the creation of the mobile app, as well as for the storage of the collected data.

In chapter 5, the main results of the developed work are presented. This includes recording ECG as well as oximeter data acquisition, including a block diagram to describe the code implemented to obtain the various quantities. It also includes the multiple layouts of the android application and an example of the visualisation of data stored in the cloud to which health professionals have access.

Lastly, chapter 6 is dedicated to highlighting the main conclusions of the present work, as well as the future required work.

Chapter 2

Cardiovascular Diseases: The Heart Failure Problem

Despite efforts carried out during the last decades, cardiovascular diseases remain one of the leading causes of deaths and disability, accounting for approximately 40% of human mortality. One of these diseases, HF, is a chronic and progressive disease in which the heart muscle is unable to pumping enough blood to achieve the body's needs for blood and oxygen (O_2) [8]. According to a study developed by Fonseca et al. [9], the number of patients diagnosed with HF in Portugal will increase about 7% in 2018, 30% in 2035 and 33% in 2060 when compared to the data concerning 2011 (Figure 2.1). In the world field, this medical condition remains one of the most common, costly, disabling, and deadly diseases, affecting more than 25 million people worldwide.

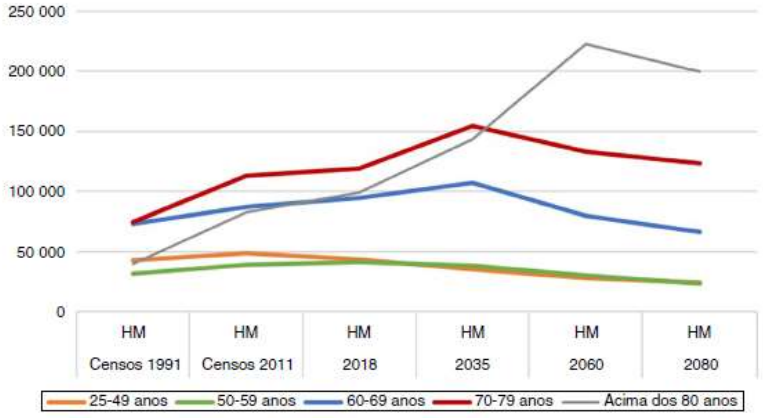

Figure 2.1 - Estimated evolution of patients with HF in Portugal by age group. Adapted from [9].

In economic terms, HF also signifies a considerable burden to healthcare systems being responsible for costs of more than $108 billion (US dollars) per year in global economics [10]. In 2012, a study conducted in the International Centre for Circulatory Health at Imperial College London estimates that, in the 24 members States of European Union, the costs related to HF in one year was about €29 billion [11]. More than that, the European Cardiovascular Disease Statistics 2017 identify HF as a leading cause for hospital admissions, requiring on average longer stays in hospital than heart attacks [12]. In Portugal, official data from 1998 reveals that the hospitalisations due to HF have an approximate cost of €24 million. However, if we considered that it passes more than 20 years, that the number of patients diagnosed with HF always increase, and that exists more sophistication in health treatments, probably this value in now substantially higher [13].

According to Cardiologists, HF is commonly classified into two types: diastolic **(DIA)** and systolic **(SYS)**. The first one, **DIA** HF, is associated with concentric hypertrophy, a thickening of the ventricular wall, which results in the reduced filling. On the other way, S**YS** HF is related with eccentric hypertrophy, a dilation of the ventricles, which manifests itself in reduced pump function. Both conditions eventually result in decreased cardiac output, increased risk of cardiac arrest, and insufficient blood supply to the rest of the body [14].

2.1 | Heart Failure Diagnosis

As said before, HF is described as the incapacity of the heart to provide the peripheral tissues with the necessary amount of blood and O_2 [8]. As cardiac output (CO) decreases because of stresses placed on the myocardium, activation of the sympathetic nervous and renin-angiotensin-aldosterone systems increases BP (for tissue perfusion) and blood volume (BV) (enhancing preload, stroke volume, and CO by the Frank-Starling mechanism). These compensatory systems can also evolve to further myocardial deterioration and deteriorating myocardial contractility. As consequences of this condition, patients reveal several symptoms, such as dyspnoea or fatigue, and other signs such as elevated jugular venous pressure, tachycardia or pericardial oedema [15].

Although there are no symptoms or clinical history signals that indicate with certainty the existences of HF, some factors are useful to indicate this condition. To help the diagnosis of this disease, the European Society of Cardiology guidelines warrant the presence of symptoms and signs (Table 2.1 and Table 2.2), objective evidence of cardiac dysfunction, and, in case of remaining doubt, a favourable response to treatment directed towards HF [16]. More detailed, the diagnosis of this disease typically involves history and physical examination, complemented with laboratory testing. Figure 2.2 shows an algorithm for the evaluation and diagnosis of HF. The initial phase, the clinical assessment, relate HF symptoms with other alternative causes, and intends to identify alternative or reversible causes of HF, and confirm its presence. To complement this first evaluation, several exams are typically performed. Among them stand out Chest Radiography and ECG, that should be performed to assess left ventricular ejection fraction when HF is suspected or if DIA HF is still suspected when SYS HF is ruled out. To asses this, a calculation is performed during an ECG, called the ejection fraction, that is used to

determine how well the heart pumps on each beat [17]. To conclude the clinical decision about the patient disease, usually doctors resort to some diagnostic conditions, namely Framingham criteria, that are widely accepted [15].

Table 2.1 - Definition of heart failure by the European Society of Cardiology. Adapted from [16].

Symptoms	**Signs**
Dyspnoea (on exertion, nocturnal)	Oedema, ascites
Reduced exercise tolerance	Elevated jugular venous pressure
Fatigue, lethargy	Crepitations or wheeze
Orthopnoea	Tachycardia
Nocturnal cough	Third heart sound, murmurs
Wheeze	Hepatomegaly
Anorexia	Displaced apex beat
Confusion/delirium (elderly	Cachexia and muscle wasting

Table 2.2 - Heart failure symptoms and signs. Adapted from [16].

I. Symptoms of heart failure (at rest or during exercise) *
II. Objective evidence (preferably by echocardiography) of cardiac dysfunction (systolic and/or diastolic) at rest and in cases where the diagnosis is in doubt *
III. Response to treatment directed towards heart failure
*Criteria I and II should be fulfilled in all cases.

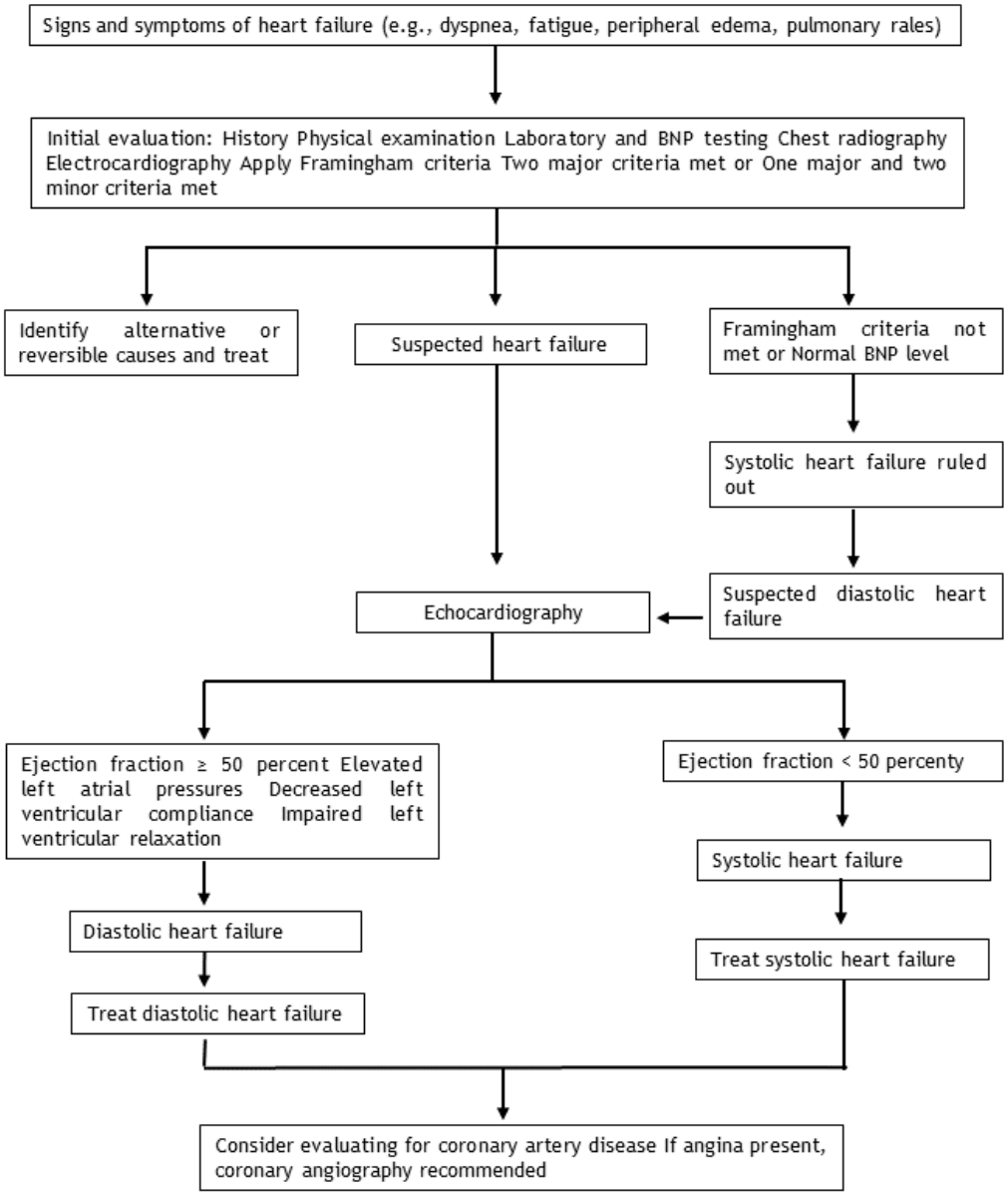

Figure 2.2 - Algorithm for the evaluation and diagnosis of heart failure. (BNP = B-type natriuretic peptide. Adapted from (8).

2.2 | Heart Failure Treatment

Currently, the treatment of HF has two dimensions, one that is pharmacological and the other non-pharmacological, which is based on the development of self-care competences. The pharmacological treatment of HF is based mainly on the recommendations of the American and European Societies, using different drugs such as diuretics, angiotensin-converting enzyme inhibitors, beta-blockers, aldosterone, spironolactone and digitalis. In the acute phase of the

disease, the institution of O_2 therapy and the administration of intravenous drugs as vasodilators, vasopressors, opioids, and diuretics are standard. Beyond this, in some cases, doctors recommend surgery to treat the underlying problem that led to HF. These surgeries involve, among others, coronary bypass surgery, implantable cardioverter-defibrillators, and cardiac resynchronisation therapy [18].

The evidence shows that the causes of hospitalisation of HF clients are usually associated with insufficient self-care practices, which result from ineffective management of the therapeutic regimen; and leading to imbalances in the health condition that are at the origin of the episodes of emergency and hospitalisation resources. Clinical pictures associated with decompensated HF are one of the leading causes of hospitalisations worldwide, representing a large part of health expenditures, which is why their eviction can contribute to the optimisation of health resources [19]. The lack of self-care skills in these clients leads to high consumption of hospital resources, due to exacerbation and consequent use of emergency and hospitalisation services [20].

Although it is a fundamental part of the treatment, people with HF face critical obstacles to take care of themselves, including physical limitations, lack of knowledge about the disease, and difficulty in obtaining social and emotional support [7]. The evaluation, the monitoring and prevention of several symptoms is an essential way of improving disease control and treatment [2]. Therefore, it is necessary to create tools to facilitate this task for both patients and possible caregivers.

2.3 | Biomedical Parameters

To promote the best possible treatment for patients with HF, the constant monitoring of several biomedical parameters is necessary, giving the clinician a more complete and accurate indication of the disease state. Several studies prove that close clinical monitoring of patients with chronic HF significantly decreases hospitalisation risk and improves quality of life [21, 22]. Usually, this clinical monitoring is achieved by frequent physical assessments. However, and using the advances of technology, remote monitoring is now a reality, accompanied by numerous advantages.

Considering the causes and symptoms of HF, several indicators can be defined for an efficient monitorization. Naturally, HR and BP were chosen directly due to their quantitative nature. The most complex phenomena are translated into available parameters. Shortness of breath translates into oxygen saturation (SO_2), and the occurrence of pulmonary oedema into thoracic fluid volume, as well as ingested NaCl due to its implication in the treatment. The parameters and proper monitoring approaches are described below.

2.3.1 | Heart rate

Heart rate (HR) is a direct indicator of myocardial performance, coronary blood flow and myocardial O_2 demand and, as can be seen in Figure 2.3, affects outcomes of nearly all stages of cardiovascular disease, including atherosclerosis, hypertension (HP), myocardial infarction (MI) and HF [23].

Several factors contribute to the beneficial effect of HR reduction in HF. This decrease regulates the energy needs of the myocardium, improving the availability of high-energy phosphates and myocardial metabolism, and reduces the production of cytokines and free radicals as well as vasoconstriction as well. Furthermore, the force-frequency ratio is essential in the regulation of cardiac function. The strength of contraction of healthy papillary muscle increases with HR, whereas in HF, it decreases. Accordingly, the raised HR in HF diminishes myocardial inotropic property, whereas its decrease will improve it. Another factor is the increased aortic stiffness in HF, which by modifying the pressure-volume relationship, amplifies the afterload. Reducing HR improves aortic compliance and elastance, limiting the afterload and the ventricular remodelling. B-blockers were proven in numerous trials in patients with HF to reduce cardiovascular mortality, emphasising the relationship between lower HR, and decreased mortality [24].

Concerning HF, the correlation between HR and cardiovascular morbidity, mortality or hospitalisation is particularly strong. When HR is equal to or higher than 70 beats per min (bpm) carries a relevant prognostic weight [24]. If considering the numbers, the risk of cardiovascular death and HF hospitalisation increased by 3% for every bpm above the resting HR and by 16% for every five bpm increase [23].

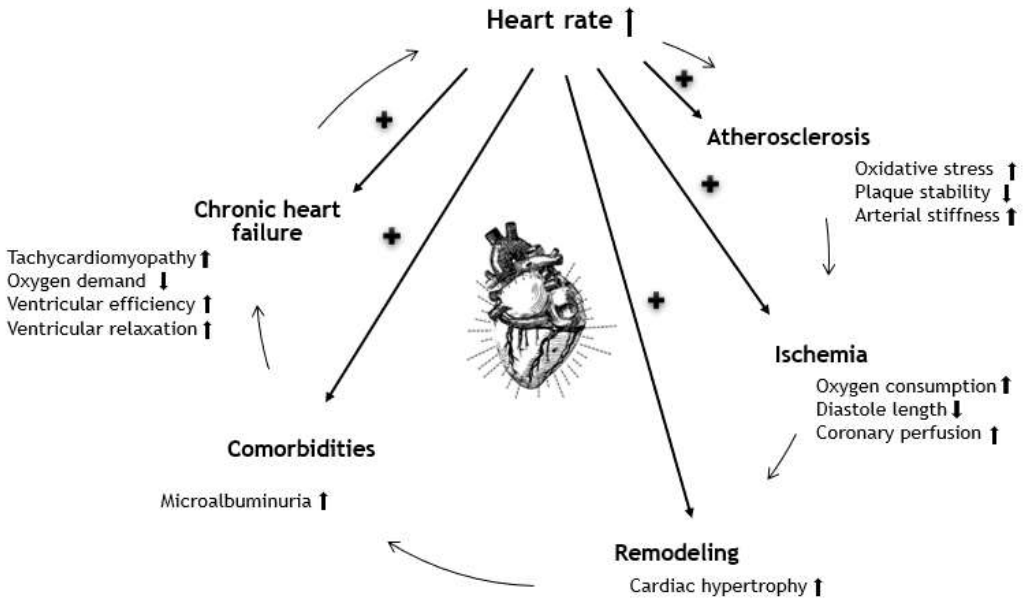

Figure 2.3 - The role of HR in cardiovascular disease. Adapted from [23].

Taking this into account, HR monitoring reveals to be an essential aspect to control in patients with HF.

2.3.2 | Blood pressure

Blood pressure (BP) is defined as a measure of the force that the hearts use to pump blood around a body. This amount is recorded as two numbers: SYS BP, that indicates the BP exerting against artery walls when the heart beats and DIA BP, that shows how much pressure the blood is using against artery walls while the heart is resting between beats. To be considered in the normal BP range, the number should be less than 120/80 mm Hg (Table 2.3). Although there are many causes of BP variation, HP is a common comorbidity in patients with HF [25]. In fact, according to Goyal et al. [26], arterial HP is one of the most common comorbidities and precursors of HF diagnosis.

Despite HP and HF are radically different conditions, the existence of a close association between them is evident. This correlation starts with HP, which is the principal risk factor for the development of left ventricular hypertrophy (LVH) and for MI, which is a common precursor to left ventricular SYS dysfunction. LVH leads more directly to ventricular DIA dysfunction, which in turn may progress to the emergence of HF symptoms [26]. Having this in the account, the measure of BP is an essential parameter in the HF control.

Table 2.3 - Blood Pressure. Adapted from [25].

Blood pressure category	**Systolic mm Hg (upper number)**		**Diastolic mm Hg (lower number)**
Normal	Less than 120	and	Less than 80
Elevated	120 - 129	and	Less than 80
High blood pressure (hypertension) stage 1	130 - 139	or	80-89
High blood pressure (hypertension) stage 2	140 or higher	or	90 or higher
Hypertensive crisis (consult your doctor immediately)	Higher than 140	and /or	Higher than 12o

2.3.3 | Transthoracic fluid volume

Pulmonary congestion, a consequence from elevated left atrial and left ventricular filling pressures, is the most common event requiring HF hospitalisation. Symptoms leading to HF hospitalisation usually occur late in the course of decompensation. Therefore, reliable means for chronic fluid status monitoring are needed to detect early decompensation.

As can be seen in Figure 2.4, the kidney acts as an early responder to the myocardial dysfunction and resulting in arterial underfilling with a decrease in circulating BV. This occurs in conjunction with baroreceptor initiation and neurohormonal stimulation, which further promote the retention of renal sodium and water. Even though that organ perfusion pressure is maintained in the short term by the initial sympathetic-driven vasoconstriction, a more gradual accumulation of interstitial compartment fluid also occurs which supports a compensatory expansion of intravascular plasma volume. The development of the interstitial fluid compartment with the associated growth in interstitial tissue pressure, thus, provides a basic mechanism for sustaining the compensatory expansion of intravascular volume over time [27].

Considering that only 30% to 40% of total BV resides typically in the arterial circulation, and even fewer in the presence of SYS HF, considerable overall volume expansion is required to maintain effective tissue perfusion dynamics. After a few time, this mechanism becomes detrimental with the development of pathological inappropriate BV and interstitial fluid expansion contributing to volume overload and organ congestion. The excess of volume provokes hemodynamic congestion with increased central filling pressures and the future development of symptomatic clinical obstruction. When in patients with HF, the already existent chronic volume excess causes a cycle of decompensation stimulating an answer of aggressive short-term diuretic treatment of congestive symptoms occurs, which is then followed by the gradual recurrence of fluid accumulation and fluid redistribution, which in turn promotes another cycle of decompensation [27].

A potential method to detect developing pulmonary congestion, a sign of decompensation, is to measure transthoracic electric bioimpedance (TEB), a non-invasive technique for CO measure [28]. With this method, it is possible to determine CO by detecting changes in the body's impedance to small electrical currents. Both blood and tissues present some impedance to electrical flow, which remains constant if volume and tissues' characteristics remain constant during the cardiac cycle. With each ejection, only the amount of blood within the chest changes, and the resulting change in thoracic BV causes changes in impedance, which allows the calculation of CO [29].

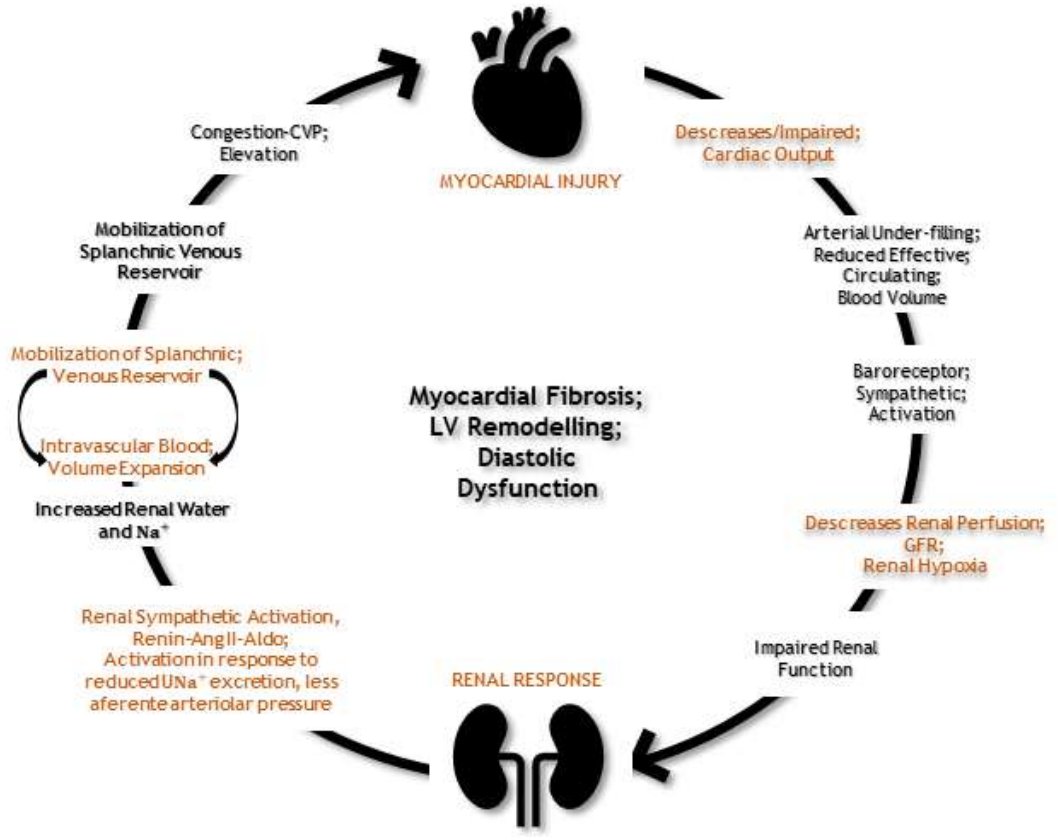

Figure 2.4 - Cardio-renal interactions in volume expansion and congestion in chronic heart failure. GFR indicates glomerular filtration rate. Adapted from (22).

2.3.4 | Oxygen saturation

Oxygen saturation (SpO_2) is an amount of how much haemoglobin (Hb) is currently bound to O_2 related to how much Hb remains unbound. In the medical field, this parameter is an essential part of the management and understanding of patient care.

Almost all biological phenomena in the human body are directly or indirectly dependent on O_2. That is because the energy stored in the form of adenosine triphosphate is produced in aerobic respiration, which only occurs in the presence of O_2 [30]. O_2 transportation from the lungs to all the cells of the body is performed by erythrocytes through the circulatory system, more particularly by the protein Hb, which is contained in those cells. When O_2 is bonded to Hb, it originates oxyhemoglobin (HbO_2). Then, when O_2 is released for the cells, it returns to Hb [30].

SpO_2 is then defined as the percentage of HbO_2 in the blood [31]:

$$SpO_2 = \frac{[HbO_2]}{[HbO_2]+[Hb]} \quad . \qquad (2.1)$$

O_2 is strongly regulated within the body because hypoxemia can lead to many acute adverse effects on individual organ systems [32]. In a healthy organism, it is maintained at a fairly stable value of about 97%. In patients with HF, the heart muscle is typically weaker and do not pumps blood the way it usually would. That means that the body does not get the needed O_2, which can cause several effects in several organs [15].

HF affects pulmonary function, gas exchange and therefore, tissue oxygenation. Having an account that lower SpO_2 had a higher rate of worsening HF events, measuring OS provides essential information about the efficiency of HF treatment [33].

2.3.5 | NaCl concentration

The human body contains many salts, being NaCl the major one. In average, an adult's body contains 250 grams distributed throughout the body, being especially plentiful in body fluids, blood, sweat, tears, semen and urine. NaCl is absorbed from the gastrointestinal tract and always brings water along with it. It is the primary mineral in plasma, the fluid component of blood, and in the fluids that bathe the body's cells. Without enough sodium, all these fluids would lose their water, causing dehydration, low BP, and death [34].

When in normal circumstances, the body sodium content is regulated by the kidney, balancing its excretion against intake. In HF, this regulation fails, and sodium nearly disappears from urine. In a study published by Haugen [35], some patients demonstrated that the sweat glands expel almost all the dietary sodium. By knowing its concentration in sudation, a correlation with the sodium intake can be attempted, which would be valuable in the control of diuretic medicines, usually prescribed in the treatment of oedemas. To the detection of sodium concentration, current methods use techniques based on stimulating sudation, followed by collecting it for electrolyte analysis [34].

2.4 | Final remarks

Taking into account the existing treatment for HF, and the importance of effective self-monitoring for the patients, the determination of which indicators allow for more effective control of patients with HF is crucial.

In other words, with the measure of all these biomedical parameters, the treatment of the patients with HF will become more effective and controlled. The goal is the real-time monitoring of HR, thoracic water and basal intrapulmonary water versus congestive. This information, together with the notion of eliminated NaCl, will allow a more efficient handling of certain drugs used in HF treatment, leading to a better recovery, and to a significant

reduction of the costs associated with the treatment of this type of pathology (due to the expected decline in the rate of rehospitalization and/or exacerbations) [33].

Chapter 3

Self-Monitoring in Heart Failure

Associated with autonomy, independence and individual responsibility for healthy behaviours, the self-care concept has evolved over the years. In the case of patients with HF, self-monitoring is a crucial component to the success of their chronic treatment but may not be feasible. The main reason for this difficulty is related to the cognitive dysfunction of a significant percentage of patients. It is, therefore, essential that health professionals can follow HF patients efficiently. Outpatient follow-up of chronic HF patients was shown to be cost-effective, even when involving home visits by health professionals, and was associated with lower rates of rehospitalisation and mortality [3, 36].

3.1 | Biomedical Sensors

Taking into account the essential biomedical parameters mentioned in the previous chapter, several sensors should be studied to achieve this measurement. Having said that, the main principles of the sensors necessary for the device development are listed in the points below.

3.1.1 | Electrocardiographic Sensor

As is well known, it is imperative to control cardiac rate and arrhythmic behaviour in patients with HF [37]. To obtain this data, an electrocardiogram (ECG) is typically performed,

using electrodes placed on the skin to measure electric variations [38]. A heartbeat is a complex series of procedures that take place inside and around the heart. The heart is a muscle that contracts rhythmically. These contractions have its beginning at the atrial side node, that acts as a natural pacemaker, and propagates to the rest of the body. This propagation leads to an electrical current on the surface of the body, that leads to an electrical potential of the skin surface [39].

An ECG device is composed of four main elements: electrodes, amplifiers, connective wires and a device with software able to process the acquired voltages. To obtain an interpretative signal, the potential difference between two electrodes is usually enhanced with the aid of an instrumentation amplifier, followed by a high-pass filter and, as a second stage, an antialiasing low-pass filter. The graphical registration of this treated electrical potential that is called ECG [40]. The standard ECG period, represented in Figure 3.1, is composed of a P wave, a QRS complex, and a T wave. The QRS complex is often three separate waves: the Q wave, the R wave, and the S wave [40].

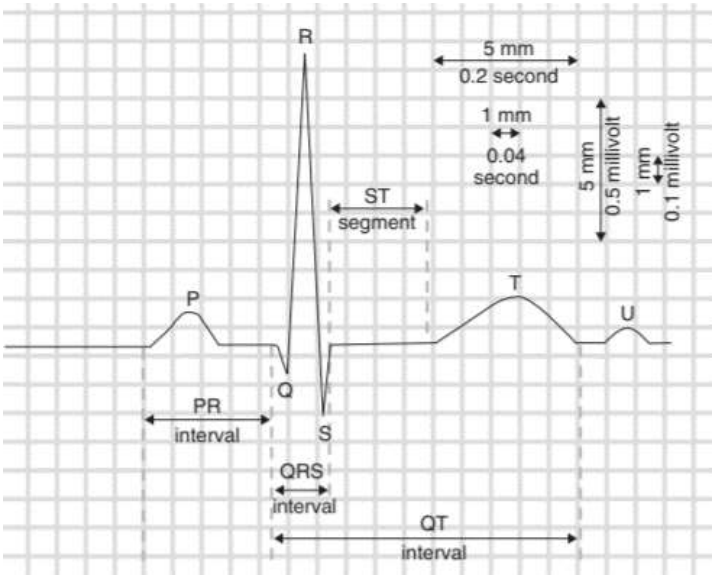

Figure 3.1 - Representation of an ECG signal - P wave, QRS complex and T wave [41].

The P wave is caused by electrical potentials generated when the atria depolarise before an atrial contraction begins — the potentials generated during ventricular depolarisation before contraction causes the QRS complex. The T wave is caused by potentials generated when the ventricles recover from the state of depolarisation. Thus, the ECG is composed of two types of waves: depolarisation and repolarisation waves. Abnormal ECG will, therefore, present a different pattern related to the cardiac pathology in question. The rate of the heartbeat can be determined from an ECG. The time interval between two successive QRS complexes corresponds to the HR. The regular interval between two QRS complexes in an adult is 0,83 second, corresponding to an HR of 72 bpm [41, 42]. In figure 3.2, it is possible to find some examples of ECG abnormalities. One of them, the sinus bradycardia, is characterised by a sinus rhythm slower than the lower standard sinus rate (60 bpm).

On the other hand, the sinus tachycardia is a sinus rhythm faster than the upper normal sinus rate of 100 bpm. Atrial fibrillation has two predominant characteristics: an irregularly irregular heart rhythm and no discernible P waves. Lastly, ventricular tachycardia is a very rapid (100 to 250 bpm) series of wide-complex ventricular depolarisations [43].

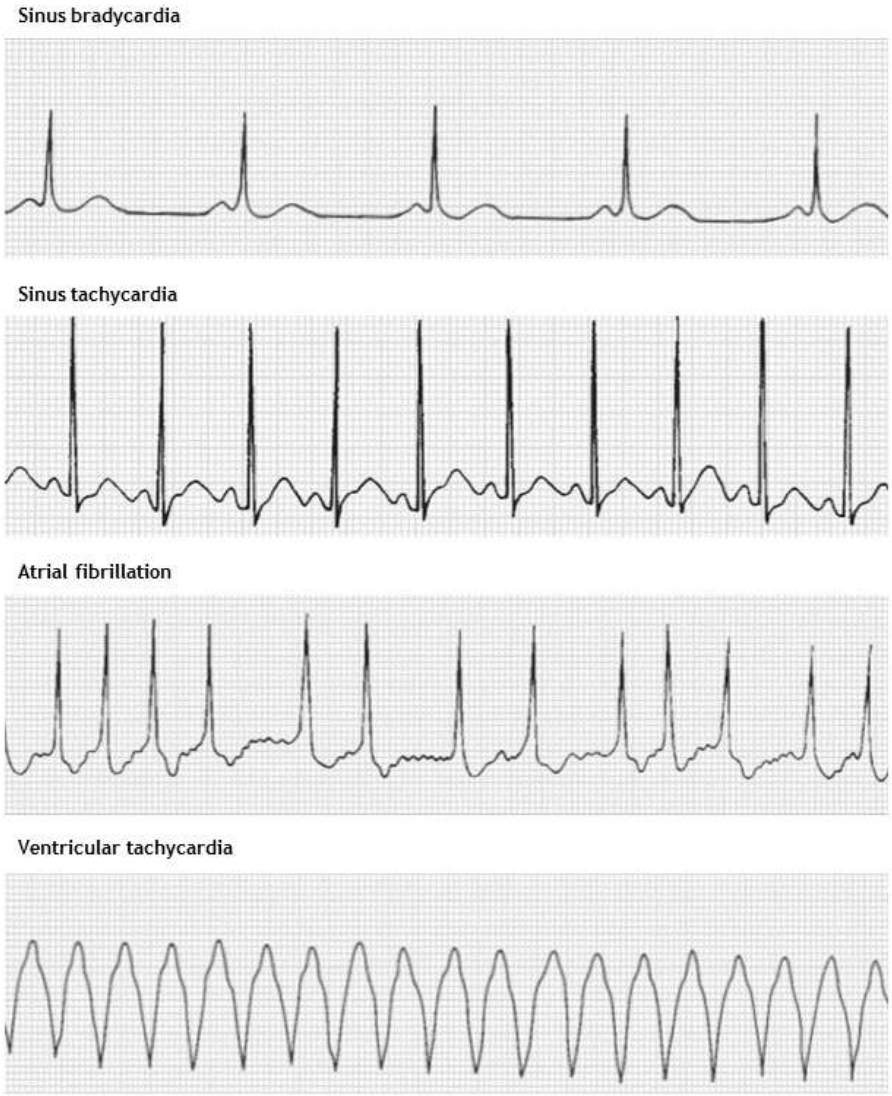

Figure 3.2 - Common ECG abnormalities [43].

The electrodes used to obtain the ECG can be placed in several different configurations, as can be seen in Figure 3.3. The simplest one uses two electrodes to measure the potential difference across only one angle, chosen from the conventional Einthoven triangle (Figure 3.4). An auxiliary electrode can be added to serve as a ground. The second one uses four electrodes to capture voltages across three angles: Lead I, II and III. A third also uses four electrodes but measures the voltage across six angles, as the additional leads (aVR aVL and aVF) can be extrapolated using the measurements of Lead I, II and III. The fourth and most complete is a

12-Lead ECG, which can be held with ten electrodes, by adding six onto the chest, whose role is to measure the action potential transversely to the heart. Finally, there are other schemes which deviate from the Einthoven triangle, such as the inverted Einthoven triangle and the vertical/horizontal configuration and can be used as an alternative to its leads [41, 44].

There are currently several alternatives on the market, including not only stationary but also wearable devices, which differ mainly by the quality of signal analysis and price.

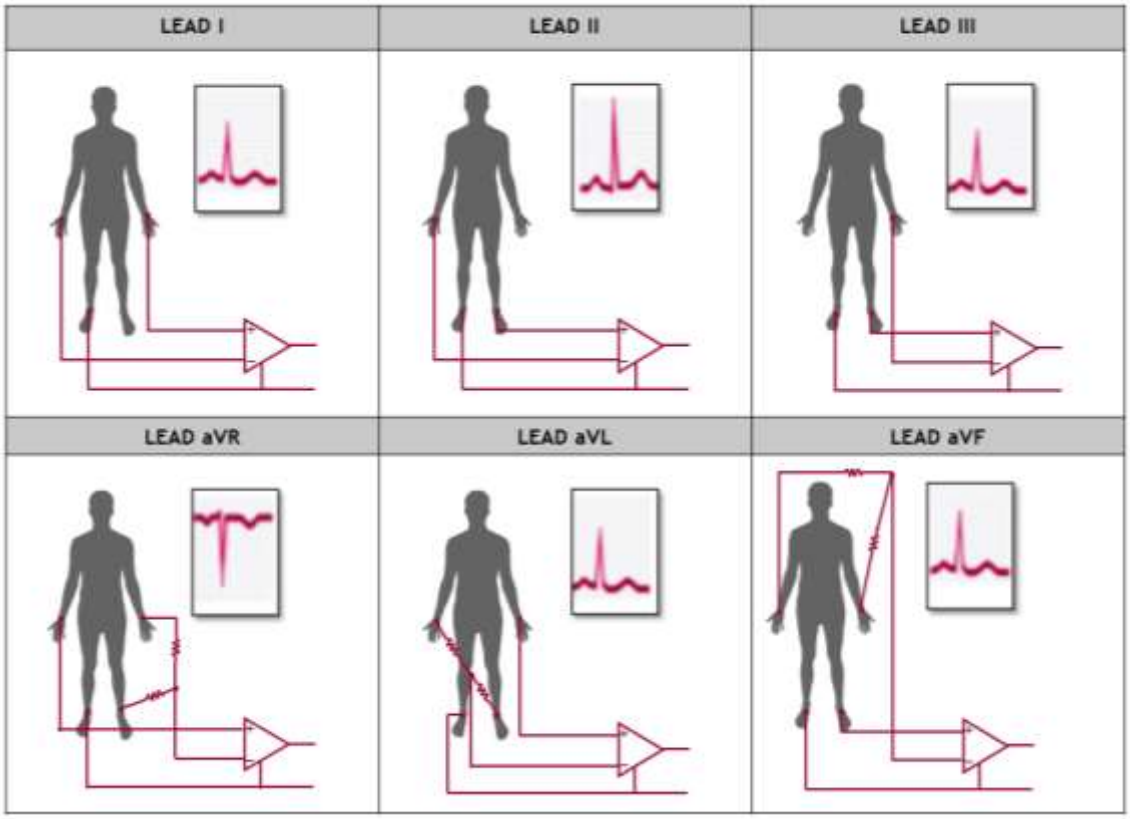

Figure 3.3 - Normal cardiac activity as manifested in the limb leads. Adapted from [41].

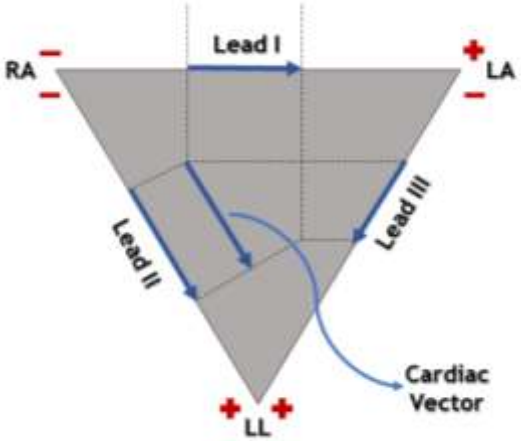

Figure 3.4 - Einthoven Triangle. Adapted from [41].

3.1.2 | Oximetry sensor

Considered a standard of care in hospitals, pulse oximetry is the assessment of SpO_2 using optical techniques, based on the different light absorption spectra of Hb and HbO_2, as the first one has higher absorption ratio at 940 nm, while the second is at 660 nm (Figure 3.5) [30].

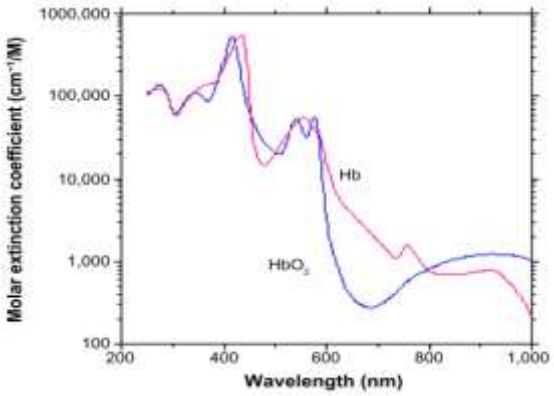

Figure 3.5 - Absorption spectra of the oxyhaemoglobin (HbO_2) and deoxygenated haemoglobin (Hb) [45].

A pulse oximeter is constituted by two light-emitting diodes (LEDs), a photosensor on the opposite side to detect light, followed by amplification and filtering of the signal acquired [46]. Pulse oximeters are usually used in the fingers, constituting a non-invasive technique. Light absorption by the tissues, venous blood and non-pulsatile arterial blood constitute the direct current (DC) component of the signal captured by the phototransistor, while the alternating current (AC) component represents the pulsatile arterial blood [30]. With the AC component, it is possible to calculate the SpO_2, bearing in mind the Beer Lambert's Law for uniform mediums:

$$I = I_0 \cdot e^{-\varepsilon(\lambda)cd} \tag{3.1}$$

where *I* is the intensity of light, I_0 the initial intensity, $\varepsilon(\lambda)$ the absorptivity of the medium as a function of the wavelength, *c* the concentration of the medium and *d* the length of the optical path. Although the blood is not a uniform medium, the errors derivate from reflection and scattering are acceptable [47]. As the pulse oximeter uses two LEDs, one emitting in the red (R) and the other in the infrared (IR) wavelengths, and assuming that both are supplied at the same distance from the phototransistor, then Δd is the same, and the Ratio of Ratios (R_{os}) can be defined as:

$$R_{OS}=\frac{\ln\left(\frac{I_{max}(\lambda_R)}{I_{min}(\lambda_R)}\right)}{\ln\left(\frac{I_{max}(\lambda_{IR})}{I_{min}(\lambda_{IR})}\right)} \quad (3.2)$$

SpO_2 can be defined in the next equation

$$\mathrm{SpO}_2 = \frac{\varepsilon_{Hb}(\lambda_R)-\varepsilon_{Hb}(\lambda_{IR})\cdot R_{OS}}{\varepsilon_{Hb}(\lambda_R)-\varepsilon_{HbO_2}(\lambda_R)+\left[\varepsilon_{HbO_2}(\lambda_{IR})-\varepsilon_{Hb}(\lambda_{IR})\right]\cdot R_{OS}} \ , \quad (3.3)$$

where $\varepsilon_{Hb}(\lambda_R)$ and $\varepsilon_{Hb}(\lambda_{IR})$ represent, respectively, the absorptivity of the Hb as a function of the R and IR wavelengths, and $\varepsilon_{HbO_2}(\lambda_R)$ and $\varepsilon_{HbO_2}(\lambda_{IR})$ represent the same but for HbO_2.

Taking into account self-monitoring, there are wearables for fingertip oximetry approved by the Food and Drug Administration (FDA) that allow the patients to monitor their SpO_2 at home [48]. More than that, there is an increasing number of oximetry wearables relying on this type of oximetry, located in the wrist, leg, ankle, forehead and chest. These wearables are connected to apps that process and store the collected data. It is imperative to reference that most of the available medical wearables are not considered medical devices. They have not been characterised in terms of reliability, measurement accuracy, safety and efficacy. An extremely low number of wearable devices have CE or FDA approvals [49].

3.1.3 | Sensors of electrical bioimpedance

As said before, TEB is a non-invasive method of measuring thoracic bioimpedance. Simplifying, impedance is a measure of the effective resistance to current flow through the body by applying a small alternating current. If we look to Ohm's law, it is possible to observe that when a known electrical current is passed through human tissue, the bioimpedance can be obtained by measuring the voltage drop between two points on the body. As the considered body region is the thorax, the measurement of this potential difference corresponds to a one lead ECG. If an appropriate model is used to describe the biological system, the volume of thoracic fluid can be estimated by measuring bioimpedance [24].

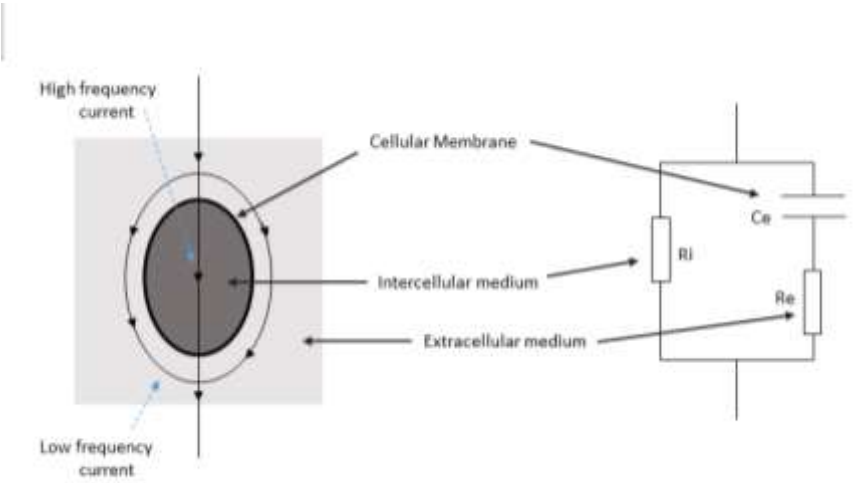

Figure 3.6 - Fricke's cell suspension electrical model and the correspondent circuit representation.

To penetrate the cell membranes, a high-frequency signal is necessary, whereas a low-frequency input only characterises extracellular impedance. In 1933, H. Fricke presented the electrical equivalent model of blood cells (Figure 3.6), which assumes that the cells are suspended in the extracellular medium with electrical properties (54). More recent, and to generalise the Fricke's model to the case where tissues contain different types of cells, the frequency-dependent behaviour of tissues bioimpedance is described by the Cole-Cole model. In this equation, it is possible to identify the parameters reflect extracellularly (Re) and intracellular (Ri) fluids resistance, the capacitive behaviour of the cell membranes (Cm), and tissue heterogeneity (α) [50].

$$Z(f) = (Re\,||Ri + Re - (Re||Ri)1 + (j2\pi f(Re + Ri)Cm)\alpha) \tag{3.4}$$

Analysing the equation, it is possible to conclude that Thoracic fluid accumulation affects directly the value of Re, which is expected to decrease with the HF worsening [51]. Taking into account the cylindrical model as being the more representative of the thorax, the volume can be determined by next equation, where V is the fluid volume, H the height, ρ is the fluid resistivity, and K is a dimensionless shape factor obtained from statistical anatomical measurements in adults, according to the chosen model [50].

$$R = K\rho H2\,\mathrm{V}R \tag{3.5}$$

Compared to the high resistivity of thoracic tissue (ρ = 200-5000 Ωcm), blood and fluid (ρ = 65-150 Ωcm) provide much lower resistance to current, which in humans should be of a low level to prevent tissue damage. Therefore, the lower impedance values should be found in regions with higher blood or fluid content, whereas higher values should be found in areas with more solid tissue. It is based on this principle that hemodynamic measurements and changes in fluid accumulation have been evaluated [52].

Recent approaches have been developed, of which can be highlighted a non-invasive wearable fluid accumulation vest/band prototypes, designed to measure TEB from four electrodes, along the thorax. The two outer pairs of electrodes located on either side of the chest and neck are used to apply a sinusoidal current (1kHz to 1MHz, 1–4 mA rms), at 16 frequencies sequentially every 0.2 seconds [53]. The voltage drop is measured by the inner electrode pair, as shown in Figure 3.7 [54]. Among the developments in these sensors, the possibility of using four electrodes along the thorax, non-invasive, and capable of measuring TEB is shown, as can be observed in figure 12 [54]. This prototype is then connected to an electronic module, which communicates wirelessly with a mobile app being the results stored on a cloud server.

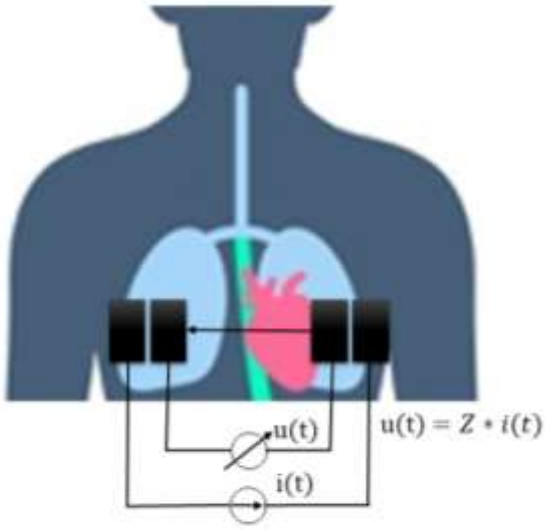

Figure 3.7 - Outer vs inner electrodes. Adapted from [54].

3.1.4 | Abdominal aortic pulse/flow sensor

As previously mentioned, BP control is essential in patients with HF. This value can be obtained through invasive methods, such as intra-arterial BP, or non-invasive, with a sphygmomanometer. This non-invasive method is already often used in self-monitoring, but it has some disadvantages compared to invasive techniques. One of the main problems is due to the impossibility of continuous monitoring, which means that short-term changes are not detected [55].

Another used method, the Pulse Wave Velocity (PWV) technique, allows a continuous, non-invasive estimation of the BP. Considering that in a living cardiovascular system, the increase in BP is associated with a growing PWV. At each cardiac cycle, the opening of the aortic valve generates a pressure pulse that propagates along the walls of the arterial tree. The velocity at which this wall-distending wave propagates is referred to as PWV, and in humans typically ranges from 4 m/s in large elastic arteries, to 30 m/s in small muscle arteries [56].

By using the next equation, it is possible to calculate the PWV, since it relates to Pulse Transit Time (PTT) of a pressure pulse along a fixed arterial segment of length D. Since D is constant, increases in BP are then easily measured by observing decreases in PTT [57].

$$PWV = \frac{D}{PTT} \tag{3.6}$$

Studies in this area also consider that PTT is the time delay between the R peak in ECG and the peak pulse in finger PPG, which shows a reasonably good correlation with SYS BP [58]. It is thus possible to relate the PTT linearly to the BP, as shown in equation 2, where B coefficient is obtained by curve fitting based on the correlation between the BP values measured with a sphygmomanometer and the associated PTT values, at different physical effort situations.

$$BP = A + B(PTT) \tag{3.7}$$

This relationship, however, can be affected by several factors, such as smoking a cigarette. This makes a constant calibration necessary [57]. Also, there is a delay between the ventricular electrical stimulation and the opening of the aortic valve, known as the Pre-Ejection Period (PEP). This fact leads to the existence of a significant error when using the R from ECG peak to estimate when blood pulse leaves the heart has a significant error associated.

In a study conducted by Solà et al. [57], the analysis of the Impedance Cardiography (ICG) waveform is used to determine the ejection of blood from the aorta. In this study, the PTT can be calculated after eliminating the PEP component, increasing the accuracy of the SYS BP. For this increased accuracy, the arrangement of the ICG electrodes made it possible to detect the impedance change due to the ejection from the aortic valve [57].

Also, a study developed in 2015 by Adisson [59] proposed a novel PTT proxy measurement based on geometrical considerations of the arriving PPG cardiac waveform. This system only required the measurement of a single point on each cardiac beat arriving at the peripheral site. This is possible by detecting a single feature that is correlated with BP, called the slope transit time (STT), that is a slope parameter calculated from the foot to peak of the SYS waveform.

Considering that transit time varies inversely with pressure, it is expected that, during respiratory activity, vary cyclically with pressure changes. The final plethysmography waveform signal observed in practice is obtained by aggregate is an aggregation of an initial wave plus a series of reflected waves. This final PPG signal is associated with two competing temporal elements, the shorter period (P1) and the pulse period (P2) (Figure 3.8). During the arterial pressure increase that occurring in expiration, the internal pulse waves travel faster, thus reducing PTT, and are P1. At the same time, the P2 increase at the HR decrease. On the other hand, in the inhalation process, the opposite occurs: BP reduces hence P1 increases, and P2 shortens due to an increased HR. It is so possible to conclude that these two temporal effects oppose each other, which may be related to the poor results that are sometimes obtained in the calculation of BP through PTT [59].

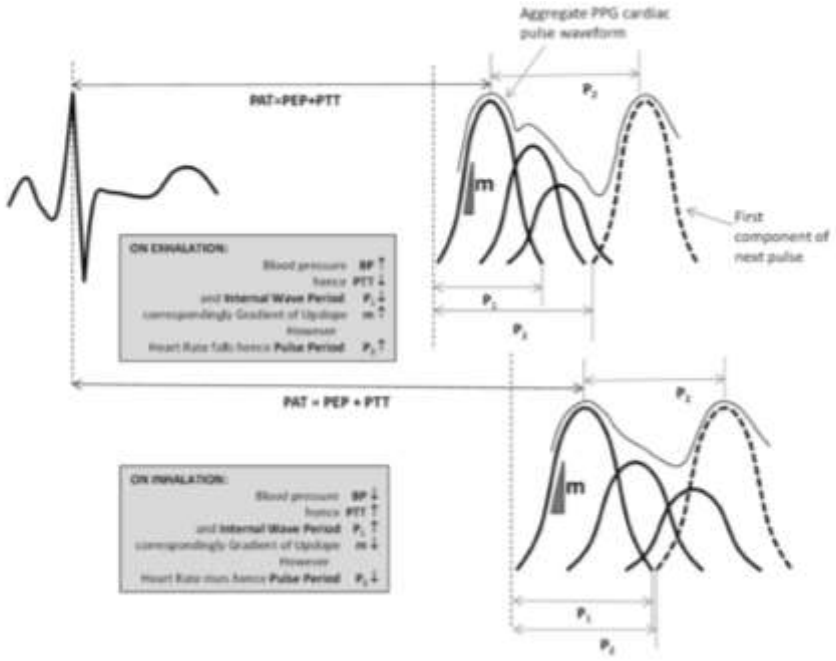

Figure 3.8 - Schematic of the opposing effects on the internal components and pulse period during the respiratory cycle [59].

Hence, as PTT increases and correspondingly P1 increases, it can be seen from geometric considerations that the gradient (m) of the upslope of the first pulse wave component should decrease. More than that, and as is known, k=1/m, being that k can be considered as a "temporal gradient", i.e., the time change per unit amplitude rather than m, which is an amplitude change per unit time. k is proportional to transit time and is not dominated by HR effects but instead follows an STT (Figure 3.9). It was therefore hypothesised that STT, and hence k, would prove a more appropriate single probe proxy for PTT. In practical terms, m can be taken as the amplitude of the first peak of the first derivative of the PPG signal (i.e., maximum gradient of the upslope): a measure easily extracted from the current computer code and the inverse of which provides k.

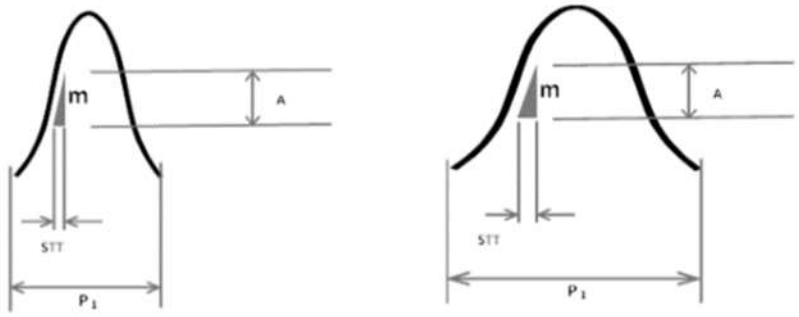

Figure 3.9 - Schematic of components of the gradient measure. k is the inverse of m and may be thought of as a 'temporal gradient'. K is proportional to the slope transit time (STT) [59].

3.1.5 | Chemical sensor for determination of sweat NaCl

The kidney is typically responsible for sodium content regulation. In patients with HF, this regulation fails, the reason why is so important the implementation of this sensor. For sodium concentration detection, current methods use techniques to stimulate sudation and collect it for electrolyte analysis. The current widely method, iontophoresis, is defined as the "faciliatory motion of ions across a membrane, permitting the transdermal delivery of vasoactive drugs" [60]. This technique introduces ionic compounds into the body through the skin by applying a local electric current.

Iontophoresis is currently one of the most widely used methods to stimulate sweat secretion. Applying an electric current through the introduction of ionic compounds into the body through the skin allows to collect and analyse excessive sweating. This conventional procedure implies the accomplishment of the several stages, namely stimulation, collection, and analysis, in separate steps. This makes it impossible to get results in real-time; wearable alternatives have been developed that make this possible.

As Figure 3.10 shows, it is possible to find an example of a platform used for self-monitoring, which makes the physiologically rich sweat sample accessible. This platform is composed of an electrode array, containing the sweat induction and sensing electrodes, integrated with a flexible wireless printed circuit board (FPCB) (Figure 3.10 A). The electrodes were patterned on a mechanically flexible polyethene terephthalate (PET) substrate to form a stable sensor-skin contact (Figure 3.10 B) [61].

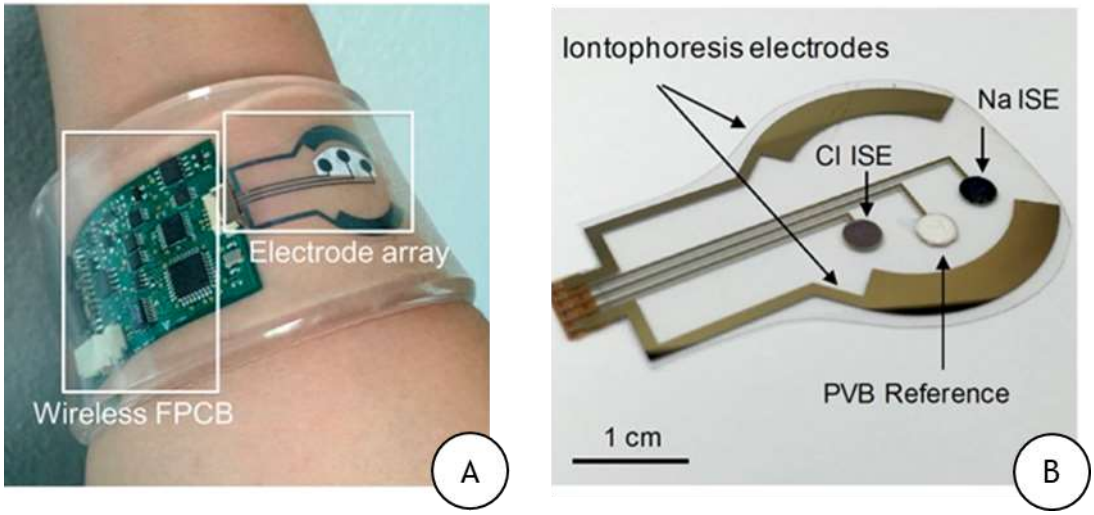

Figure 3.10 - A | Image of the autonomous sweat extraction and sensing platform. B| Image of iontophoresis and sweat sensor electrodes for Na+ and Cl- sensing [61].

Looking at Figure 3.11A, it is possible to see that through the electrical decoupling of the switchable sweat and sweat induction modes of operation, it is possible to preserve the independent functionality of the individual sensors and the iontophoresis process. Composed of a programmable current source for the iontophoresis current and a protection circuit that establishes an upper limit in the iontophoresis current, the sweat induction circuit can prevent overheating and subsequent burning of the skin. The sensors are then able to quantify sweat Na +, Cl-, and glucose, which makes this system quite interesting for home self-monitoring. By looking at Figure 3.11 B, it is possible to have an overview and summary of the modes of induction and detection of the operation [61].

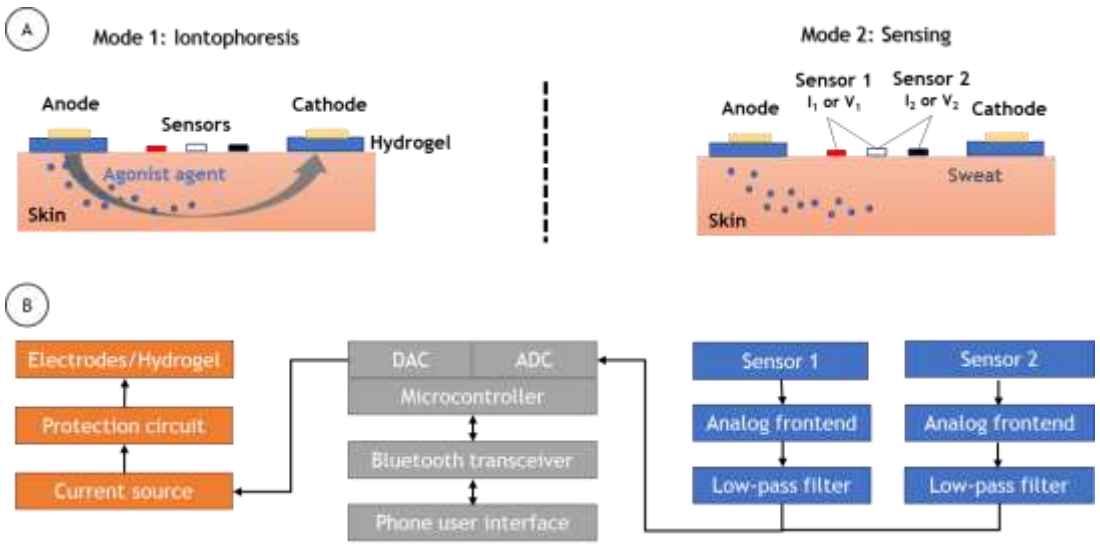

Figure 3.11 - Schematic illustration of the iontophoresis and sensing modes and system-level block diagram of the platform showing the iontophoresis and sensing circuits. Adapted from [61].

3.2 | Existing Devices

Being one of the main fields in the telemedicine applications, there are already several monitoring systems for HF patients, mostly by the implantation of cardiac devices, like the CardioMEMS™. However, these devices are invasive, which is why there are also several systems that use non-invasive sensors, such as the ECG or the oximeter. The following subsections introduce a summary of implantable and non-implantable devices used in HF monitoring.

3.2.1 – Implantable monitoring devices

Regarding implantable monitoring devices, these can be divided into two types: secondary monitoring devices, that provide information in addition to their original therapeutic function through the addition of sensors and primary monitoring devices, that can be used solely for monitoring [5]. The secondary monitoring devices are a complement to use in patients who have an implantable cardioverter-defibrillator or pacing devices with added monitoring capabilities. The constraints provided include ECG analysis, frequency of shocks, 'contractility' through a pacing lead, intrathoracic impedance and other parameters as possible indicators of impending volume overload [62].

Concerning primary implantable devices, they were developed to measure pressures continuously at different sites within the cardiovascular system. This goal was encouraged by the conclusion that a change in filling pressure seems to be one of the earliest indicators of imminent cardiac deterioration [5]. The HeartPOD device (Figure 3.12), from St. Jude Medical, is a wired device designed to measure left atrial pressure, is one example of these devices. The components of the invention include a wired sensor introduced trans-sceptically into the left atrium and connected to a subcutaneous antenna powered and interrogated by an external patient advisory module using radiofrequency [63].

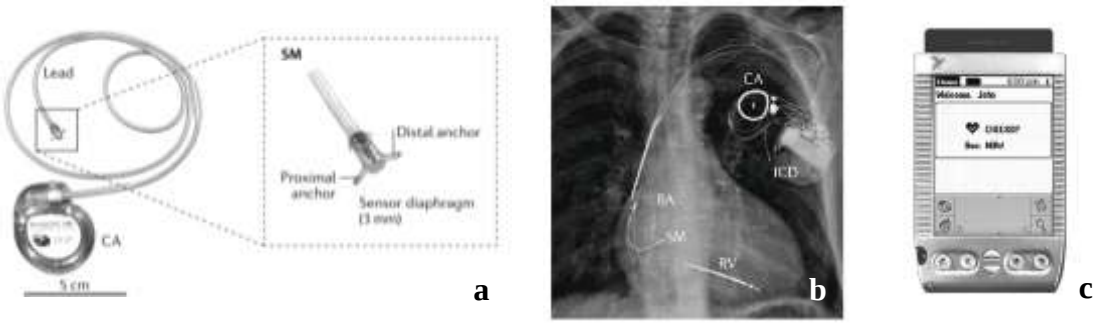

Figure 3.12 - HeartPOD device. a | Photographs showing the implantable portion of the system. b | Chest radiograph of a patient implanted with the L AP monitoring system from the left axillary vein. c | Photograph of the patient advisory module used by patients to communicate with the implanted sensor lead. Adapted from [5].

The second-generation of the implantable devices use miniaturised sensors that are all transponders and are entirely contained within a vessel or chamber. One of them, CardioMEMSTM Monitoring (Figure 3.13), is a wireless device that monitors pulmonary artery pressure (PAP) that was approved by the FDA in 2014. It is implanted in the distal pulmonary artery via the right heart catheterisation (RHC). This is the first sensor-based device which demonstrated a significantly lower risk of HF hospitalisation [64].

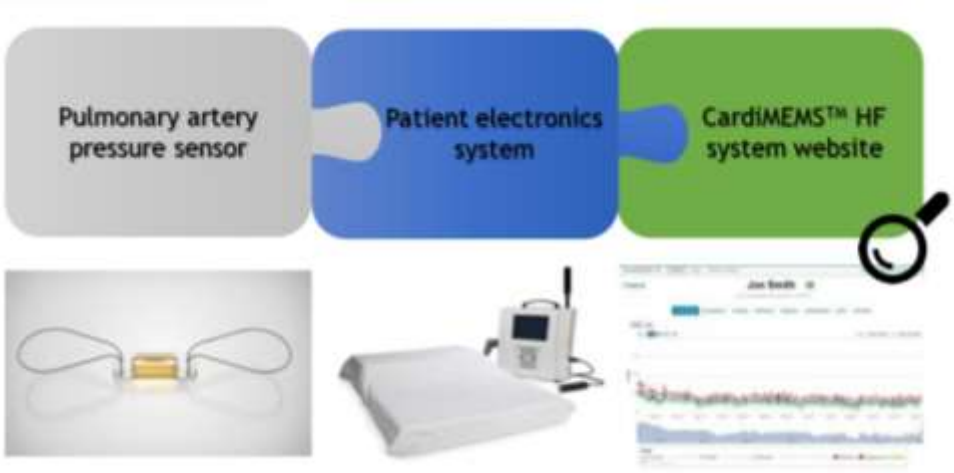

Figure 3.13 - CardioMEMSTM HF System. Adapted from [64].

Another device like CardioMEMS sensor is the Endotronix sensor, that was developed using endovascular access in a branch of the pulmonary artery. This system uses a handheld aerial positioned over the sensor site that is connected to a rechargeable, high-power transmitter-receiver, which is semi-portable, enabling readings in other body postures. The display unit informs patients that the aerial is well-positioned and can then be used to take measurements and afterwards convey treatment information to them. The device has been tested extensively in animals and is now undergoing human testing for the first time [5].

Being developed at Imperial College London, UK, The SAW device (Figure 3.14) is the only one in the public domain to use a SAW resonator and is used to monitor pressures continuously from the main pulmonary artery or one of its branches. The recordings are collected wirelessly and automatically by an external, body-worn reader, which is similar in size to a large smartphone, stores the continuous pressure recordings 24 h per day and can be interrogated in real-time through the Internet or mobile phone networks. The data set includes patient activity, as well as respiratory and haemodynamic details. The device is undergoing extensive preclinical testing in preparation for the first-in-human insertion [5].

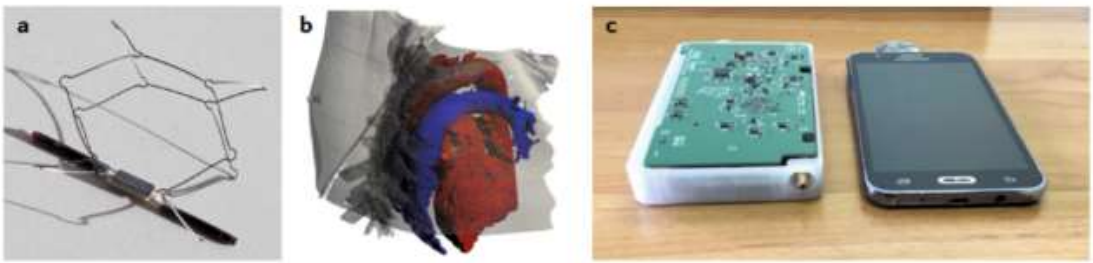

Figure 3.14 - The surface acoustic wave (SAW) system. a | Photographs of the sensor, aerial and anchor. b | Modelling the depth and orientation of the pulmonary artery. c | Wearable reader prototype and a smartphone for comparison. Adapted from [5].

3.2.2 | Non-Implantable monitoring devices

In addition to the devices mentioned in the previous section, there are also reports in the literature of several other non-invasive sensors for monitoring certain ECG variables and bioimpedance [65]; of cardiac response to exercise [54]; and even body smell [65, 66] believing that certain volatile gases released into the skin may help in the diagnosis.

The Multisensory Monitoring in Congestive HF (MUSIC) study is a prospective, multi-centre, nonrandomized study used to develop and validate a multisensory algorithm for the prediction of acute HF decompensation in HF patients, using a non-invasive multisensory adherent monitoring system. In this study, the participants were monitored for approximately 90 days with the multisensory (MUSE) system, which continuously records physiologic variables such as HR, fluid conductance, activity, and respiration. Besides these parameters, also the healthcare utilisation (hospitalisation, emergency room visit or urgent care visit requiring IV therapy) and changes in diuretics were recorded for correlation with the MUSE data. This system includes an adherent device, which attaches to a patient's torso. The adherent device is equipped with gel-coated electrodes and is connected to an electronics module that collects patient data and transmits it to a wireless modem in the patient's home. Data are sent automatically through a standard telephone line from the modem to a remote monitoring centre for analysis and storage [66].

The Sentrian Remote Patient Intelligence is a commercial machine-learning platform that allows processing data such as SpO_2, BP and temperature that come from a wireless pulse oximeter and BP monitor. This platform was evaluated on its effectivity for home monitoring of patients with congestive HF, showing success, despite some limitations mainly due to lack of patient engagement [67].

Regarding the cardiac response to exercise, a study conducted by Bombardini et al. [68] was intended to compare the sensor-based quantification with standard stress echo assessment in the post-exercise phase and to exploit the sensor-based intelligent monitoring in a larger group of exercising subjects as a model of a wireless telemedicine system. This study includes 150 patients and 22 controls, being all measurements obtained with non-invasive wearable sensors. At the end of the study, and after a continuous measure of post-exercise contractility, DIA time and pressure changes by a cutaneous sensor, it was concluded that heart disease affects not only exercise SYS performance, but also post-exercise recovery, DIA time intervals and BP changes [68].

On the other hand, a study developed by Voss et al. [69] makes the application of an e-nose system for diagnosis of HF based on the detection of disease dependent sweat volatile gases from the skin surface caused by an impaired metabolic. This study represents a new non-invasive method to identify HF, being the application of the sensor chip directly on the skin surface possible. The results of this pilot study that englobed 57 patients with HF and 28 controls suggest that an e-nose could be successfully applied for diagnosing and monitoring HF patients after analysing the human body odour from the skin surface [69].

Dovancescu et al. [51] tested the efficiency of the transmission of the measured TEB by the Philips fluid accumulation vest (FAV) to a mobile phone, to detect early stages of HF

decompensation. The FAV systems consist of a wearable device that can be used at home, which measures the TEB at multiple frequencies, the ECG, patient's motion and posture (Figure 3.15). Results regarding the use of this equipment were not reported [51].

Figure 3.15 - Components of the fluid accumulation vest (FAV) measurement system and the process for data acquisition, transfer, and storage. Adapted from [51].

On the other hand, Dias [70] developed, to capture data in a practical and non-invasive way, a wearable sensor network that can be used for gait analysis and cardiovascular surveillance. This system uses two applications: an e-legging to capture human locomotion parameters and a T-shirt to capture ECG, respiratory rhythm, and pressure. The experimental results obtained in a biomechanics laboratory, for a real-time human locomotion data acquisition show performance similar to other commercial systems, with the advantage of consuming lower wireless transmission power and having the measurement of an additional quantity: angular velocity [68].

Still in the same field, in 2016, Trindade et al. [71] developed a t-shirt prototype that embeds novel textile sensors to capture cardio and respiratory signals capture (Figure 3.16). The performance tests were realised in terms of signal-to-noise ratio amplitude and signal interfering instigated by baseline wander and motion artefacts, through laboratory tests with subjects in standing and walking conditions and using a T-shirt prototype connected to a commercial three-channel Holter monitoring device in a hospital environment. The results show that the embroidery method is adaptable and subject to integrate multiple sensors and signal processing modules to realise large surface interactive textile wearable systems, enabling the gathering of large amounts of information, still providing higher security to the user [71].

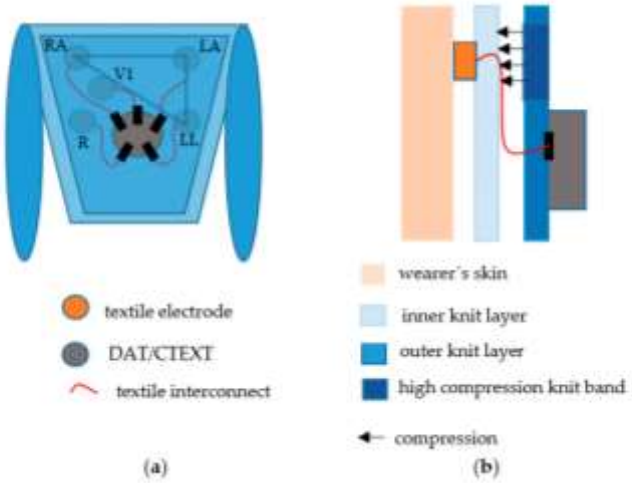

Figure 3.16 - Schematics of T-shirt embedding textile sensors, textile interconnectors and either a custom DAT unit or terminals for electrical connection to an external data acquisition unit; (a) front-view representation, and (b) cross-section representation. Adapted from [71].

Mobile Health (mHealth) apps are usually intended to help patients manage their drug intake, promote treatment adherence [72], but they can also be used as a solution for early diagnosis of heart conditions, such as atrial fibrillation. For that, the mHealth app must be able to detect and distinguish different types of arrhythmias. The advantage regarding the Holter device, which is used in the clinic, is its simpler use and the possibility of recording cardiac activities for an extended period [73]. The Heartbeats app, the AliveCor KardiaBand, the Cardiio Rhythm, the My Diagnostick, the Cardio Sense and the CPstethoscope apps were investigated to evaluate their accuracy on detecting atrial fibrillation. The most effective wrist-worn wearable devices were the Apple Watch in combination with the Alive Cor KardiaBand app [73].

3.3 | Final remarks

Taking into consideration the analysis of already existing solutions for HF remote monitoring, no such a single system exists which comprises all the sensors and captures all patient monitoring quantities that would be pertinent to our study. The most tested and validated systems are typically composed of implantable devices. Even when referring to non-invasive monitoring, it is typically accomplished with a pre-implanted sensor, or it is intended to obtain only one magnitude, which is insufficient for effective monitoring of HF patients.

Even though the real-time data generated from wearable devices to implement safer diagnosis and cardiac event detection is a powerful tool in current medicine, digital data represents some challenges, due to the complexity of achieving data quality, real-time processing and interpretation of results [74]. Considering this, the development of wearable devices is something that still has a lot to work on, until an utterly compelling system is achieved.

Chapter 4

System Architecture

The main goal of this project was the creation of a wearable HF monitoring device comprising sensors to capture different patient condition status quantities. Among the challenges inherent to the development of this project, we highlight the correct choice of sensors in order to obtain useful quality data. To achieve an efficient selection of sensors, several aspects should be considered. Table 4.1 presents some case studies to help the decision of which sensors should be used to the detection of SpO_2 level as well as the HR. According to this table, should be used a pulse plethysmograph for both measurements, even for the detection of HR. The determination of BP will be performed from these sensors, so it does not influence their choices.

Figure 4.1 - Final system architecture scheme.

In order to implement this system efficiently, it was decided to choose a hardware development platform to facilitate system development and decrease development time. This hardware selection should accomplish a set of prerequisites, described in point 4.1, taking into account the complete objective of the project, which includes the use of several sensors, Bluetooth Low Energy (BLE) communication to an android application and the storage of data in the cloud. The final scheme for the system architecture can be found in Figure 4.1.

Table 4.1 – Main remarks on choosing the best sensor to measure blood oxygen level and heart rate. Adapted from [75].

Measure blood oxygen level	Heart rate measurement
Wrong Sensor: A reflective pulse plethysmograph. Attractive because it is small, low cost, and because it can be placed almost anywhere on the body but is not accurate enough to provide medically acceptable results without expensive and inconvenient calibrating.	Wrong Sensor: While ECG electrodes provide a very good way to measure heart rate, they can be inconvenient. It is critical to have good contact, which often requires moist ECG pads, which is not acceptable for most consumer products and many medical devices. Large flexible electrodes can make good contact, but they usually require some adhesive that needs to be replaced periodically.
Right Sensor: A transmissive pulse plethysmograph, while accurate, is restricted to use on parts of the body that are thin enough to allow light to pass through. A design change allowed them to place it around a finger.	Right Sensor: A pulse plethysmograph picks up pulse as well as measuring blood oxygen. Even the reflective type can be used to measure pulse rate and can be placed on the wrist where a transmissive pulse plethysmograph would not work. While it will not provide accurate Oxygen measurement, especially during movement, it will provide an adequate measurement for many applications, and it can provide an accurate heart rate even during movement with better comfort and convenience that will encourage usage.

4.1 | Biomedical development platforms

For the creation of the intended system, it was necessary to study the possibility of adapting an existing system to help in the project development, in order to decrease the required development time. For this, it was developed an extensible research to achieve a better solution. In this investigation, several points were considered: ease of development, data acquisition, processing and storage, connectivity and power consumption, as well as physical device design and cost requirements. More than that, this system should be aimed at the quantities to be measured, having already implemented some of the sensors, or such that its implementation is feasible.

Considering all these points, a final list of the considerate devices was created (Table 4.2), which enables easy comparison of the systems considered. These platforms are further explained later.

Table 4.2 - Evaluated systems and their main sensors.

Platform development kit	Include sensors (or easy to add)
I. Maxim health sensor platform	ECG / Biopotential AFE, Pulse-Oximetry / Optical Heart-Rate Sensor, accelerometer, gyroscope, barometric pressure sensor and Human Body Temperature Sensor
II. Hexiwear	Accelerometer and Magnetometer, Gyroscope, Pressure sensor accurate up to Altitude sensing, Temperature and humidity combo, Ambient light sensor, Optical Heart rate sensor, Oximeter and ECG (click ™ boards)
III. Bitalino	Electromyography (EMG), Electrocardiography (ECG), Electrodermal Activity (EDA), Electroencephalography (EEG), Accelerometer (ACC), Light (LUX)
IV. MySignals	GSR, ECG, EMG, Spirometer, SpO_2/BLE, Blood Pressure/BLE, Airflow, Body Position, Scale

Regarding the first option, the Maxim health sensor platform solution (Figure 4.2), is an integrated sensor platform that integrates one biopotential analogue front-end solution, one pulse oximeter and heart-rate sensor, two human body temperature sensors, one 3-axis accelerometer, one 3D accelerometer and 3D gyroscope, and one absolute barometric pressure sensor. It is based on the MAX32620, an Ultra-Low-Power Arm Cortex-M4 with FPU-Based Microcontroller (MCU). As for the implementation of this platform, the principal concern was related to the implementation of the remain sensors necessary to the final project, since it was not designed for adding more sensors [76].

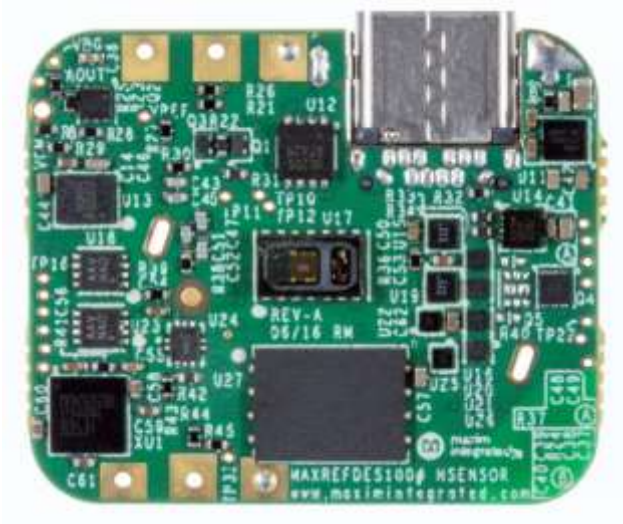

Figure 4.2 - Maxim MAXREFDES100# health sensor platform [76].

The second considered solution, the Hexiwear [77], represented in Figure 4.3 is similar to the first one. Being a development platform, it is open-source and extensible, which is very interesting for this study. More than that, and among other sensors, includes a Microcontroller NXP Kinetics K64, MK64FN1M0VDC12, com core ARM® Cortex®-M4, Bluetooth, accelerometer, gyroscope, oximeter and HR sensor, current time information. It is simply extensible using the click ™ boards, being the ECG and oximeter sensors almost ready to use.

Figure 4.3 - Hexiwear device [66].

Other considered solution, the Bitalino (Figure 4.4), this is a popular open-source biomedical development platform that has a variety of biometric sensors with an Atmega328 microcontroller for processing the sensor readings and a Bluetooth module for wireless communication. Some of those sensors include Electromyography (EMG) sensor, ECG sensor, LUX sensor, Accelerometer and Electro Dermal Activity (EDA) sensor. Similar to the previous

platform, each module is separated in blocks, that can be removed in order to customise the setup depending on what we want to measure [78].

Figure 4.4 - Bitalino Development kit [78].

The fourth option, MySignals, is an open-source sensor platform that offers a wide range of bio-signal sensing capabilities to open-source hardware platforms. This system allows the measurement of more than 20 biometric parameters, such as pulse, breath rate, SpO_2, ECG signals and BP. This platform can be purchased in two versions, as exemplified in Figure 4.5.

However, it has a very excessive dimension compared to the objective of this project, and it is still quite expensive, exceeding, in any case, the €1000 [79].

Figure 4.5 - MySignals development platform. A|Software development platform ready to use with the microprocessor Atmega2560. B| Hardware development platform for personalised development. Implied the utilisation of Arduino Uno [79].

Other two options were initially considered, LifeSigns and GEN II. However, the information found in the research was a little scarce, and the communication with the development company was not successful. Regarding the LifeSigns [80], it appeared to be the most well-targeted for health monitoring in terms of the variables that can be captured; However, the integration of missing sensors seems to be a complicated process, which would hinder the project development. Relatively to the last device considered, the GEN II, it is described as a sensor with many high-performance sensors and features embedded in a small wearable system. However, as said before, the specific information found was scarce.

None of these systems provides an ideal solution to implement the system hardware, always missing some of the sensors that we need to implement. Given the required investment as well as the dimensions of mySignal, these have been dropped. That said, the final comparisons were made between Maxim health sensor, Hexiwear and Bitalino.

These three platforms show similar characteristics, except that Maxim's solution only has one channel ECG and no current time. Regarding size, all of them allow the development of a system that meets the specifications. Concerning the adaptability to the needs of the project, as well as the extensibility, Hexiwear and Bitalino are the most suitable ones to aid in the development of this project, as they are both ready to receive external components. However, the Hexiwear screen is an advantage, facilitating immediate visualisation of the values. Considering this, the chosen system is Hexiwear, which is described in detail in the following point.

4.2 | Hexiwear

Hexiwear is a wearable IoT development platform developed by MikroElektronika in collaboration with NXP, aiming to be a support for projects development (Figure 4.6). It comes in compact form factor with on-board power-efficient Kinetis K64F MCU, BLE connectivity, a 1.1” OLED display, a 190mAh 2C Li-Po battery and still 8 Sensors on board, which includes 6-axis accelerometer and magnetometer combo, 3-axis gyroscope, pressure sensor, temperature and humidity combo, ambient light sensor and an optical HR sensor [66].

The choice of this equipment was due to several factors, including the fact that it is an economically viable option, comes equipped with BLE, and is feasible to communicate with iOS/Android apps and also the cloud, comes equipped with a battery and even expandability by using sensors and transceivers through Click™ boards. More than that, the already included sensors can be used as a complemented of the initial project. For example, the accelerometer measurements can be used to verify if the patients have complied with the physical activity recommended by the healthcare professional [81].

Considering the available click boards capable of obtaining the desired signals, two boards were selected to be purchased together with Hexiwear: the ECG 2 Click (ECG2C) and the Heart Rate 4 Click (HR4C), described in the next chapters. Still, for the development process, it was also acquired the Hexiwear docking station, that allows the communication between the Hexiwear and the click boards.

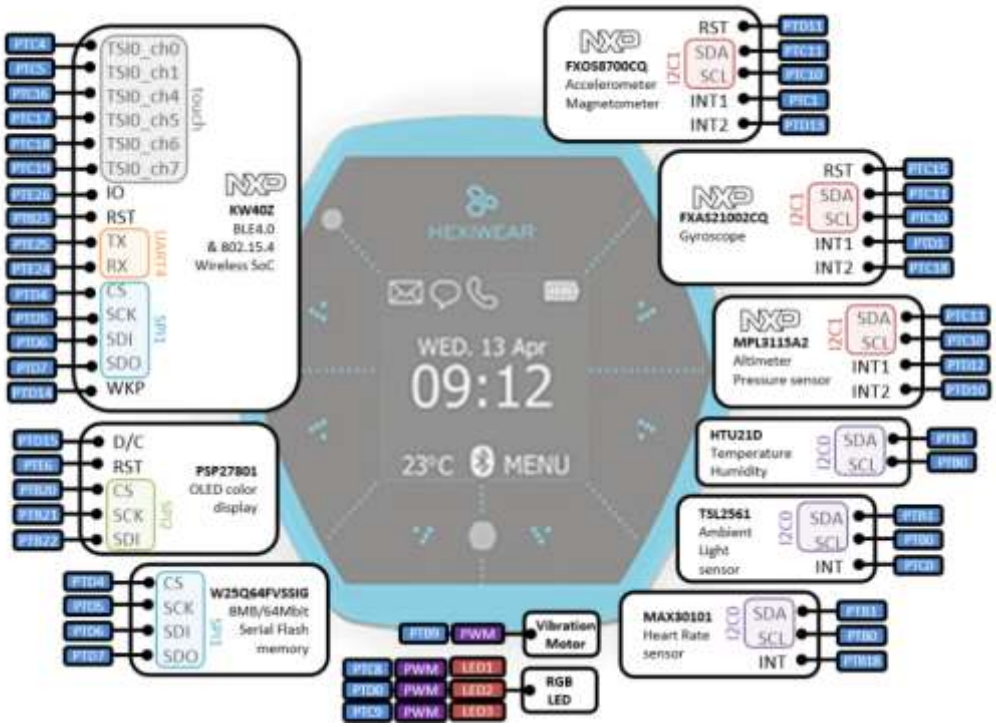

Figure 4.6 - Hexiwear Component Pinout. Adapted from [66].

4.3 | Docking Station

The addition of the external components implies the acquisition of the Hexiwear Docking Station Figure 4.7, an expansion board that provides an interface for programming, debugging and enhancing Hexiwear with additional functionalities. This device includes mikroBUS™ socket for click boards™, microSD slot, LEDs, Hexiwear connector that interfaces to Hexiwear's main MCU and Wireless MCU, I2C interface, JTAG connector for external programmers, ON/OFF switch, Pushbuttons, Micro USB port and OpenSDA control interface [82].

Figure 4.7 - Hexiwear Docking station.

4.4 | ECG 2 CLICK

Represented in Figure 4.8, the aim of ECG 2 Click (ECG2C) is the tracking of the patterns of the heart beating. This board contains an ADS1194 16-bit delta-sigma analogue-to-digital converter from Texas Instruments, a built-in programmable gain amplifier (PGA), an internal reference, and an on-board oscillator [83].

The ECG data can be obtained from two measurement options: a three-wire or a four-wire measurement. In the first one, the electrodes are placed in the left arm (LA), right arm (RA) and the left side of the abdomen (below the heart) or on the left leg. In the four-wire communication, the electrodes are placed on both arms and legs. Concerning the power supply, the ECG2C uses 3.3 V as a digital power supply, and 5 V is used for analogue power supply. It still has OverVoltage and OverCurrent protection using 22 kΩ resistors and diodes. Regarding communication, this board communicates with the target MCU over Serial Peripheral Interface (SPI) and the following mikroBUS pins: PAC, RST, PWD and DRD [68].

Figure 4.8 - ECG 2 CLICK board.

4.4.1 | SPI communication

To the comprehension of the code implementation to the communication between ECG2C and hexiwear, the main concepts associated with the SPI communication are described below.

4.4.1.1 | SPI Features

SPI is a standard communication protocol, that uses the master-slave relationship, being that the master is the controlling device (usually a microcontroller) and the slave (usually a sensor, display or memory chip) receives instructions from the master. This interface is characterised for being a full-duplex synchronous connection. The devices interconnected by SPI communicate according to a Master/Slave protocol, in which the master provides communication starts by activating the desired slave's CS (Chip Select) line and is responsible for updating the clock line (SCLK) [84].

The communication is bidirectional using the MOSI line to send data from the master to the slave and the MISO line to receive [71].

The signals to retain are:

- SCLK - clock signal that establishes the synchronism between master and slave;
- MOSI - data transmission line from master to slave. Bit rate transmission bit in sync with the flanks of the clock signal;
- MISO - data transmission line from slave to master. Bit rate transmission bit in sync with the flanks of the clock signal;
- CS or SS - slave selection line. Typically, each CS line is connected to a slave, and the master communicates with the slave associated with the active selection line.

4.4.1.2 | Master-Slave relationship

To establish a simple SPI communication, it is only needed to interconnect properly four communication lines, as can be seen in Figure 4.9.

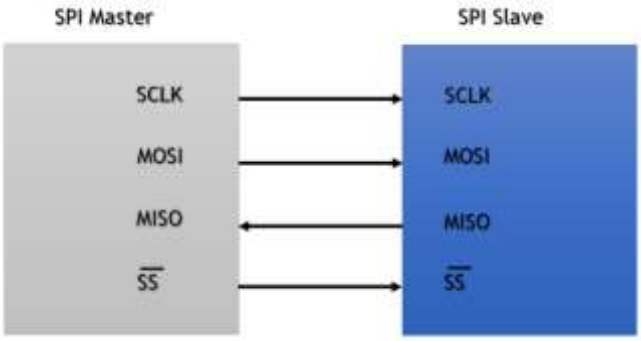

Figure 4.9 - Master-slave communication. Adapted from [71].

On the other hand, in multiple communications, several slaves can be interfaced to the master. This communication can be made point-to-point, where a different CS (SS) line is assigned to each slave. The connection is made with the slave whose selection line is active (Figure 4.10 A). Using a cooperative slave system, all slaves are active, and data are sent successively from one slave to the other (Figure 4.10 B).

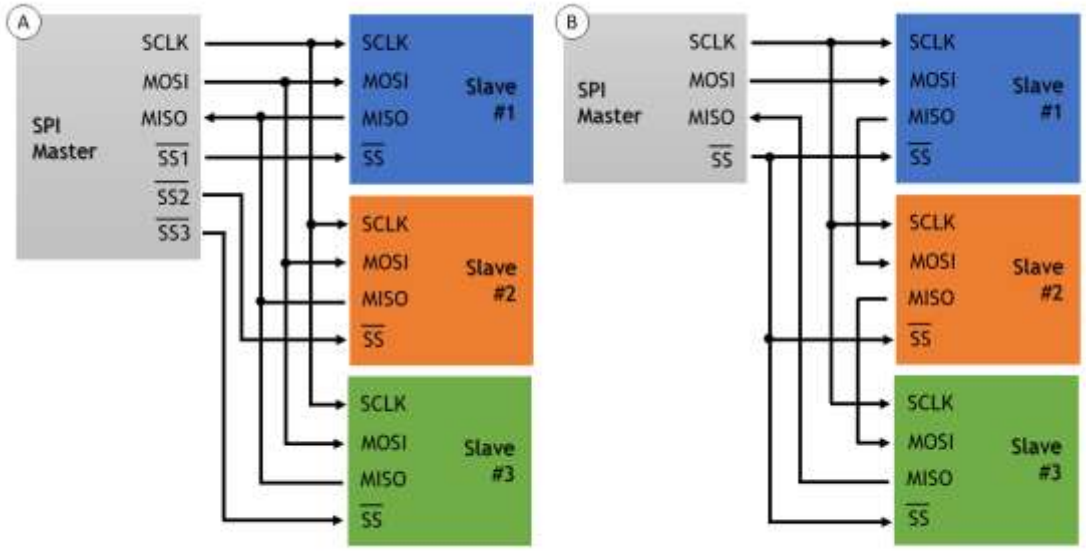

Figure 4.10 - A| Master connected to several independent slaves **B|** Master connected to several cooperative slaves. Adapted from [71].

In our design, the simple SPI connection is used as there is only one device to communicate under this protocol.

4.4.1.3 | SPI protocol state machine

The master is implemented as a finite state machine (Figure 4.11) that follows the following steps:

1. To start the communication with the slave, the master places an SS line at the logical level of zero.
2. When SS is at zero a flank is given on the SCLK line (ascending or descending configuration) and the devices update the MOSI and MISO line to the value to convey.
3. A new flank is given on the SCLK line (ascending or descending), the value on the MOSI and MISO line is read and registered.
4. Steps two and three are repeated until all bits are transmitted.
5. When the transmission is complete, the SS line is reset to the logic level one, and the master waits for a new communication order.

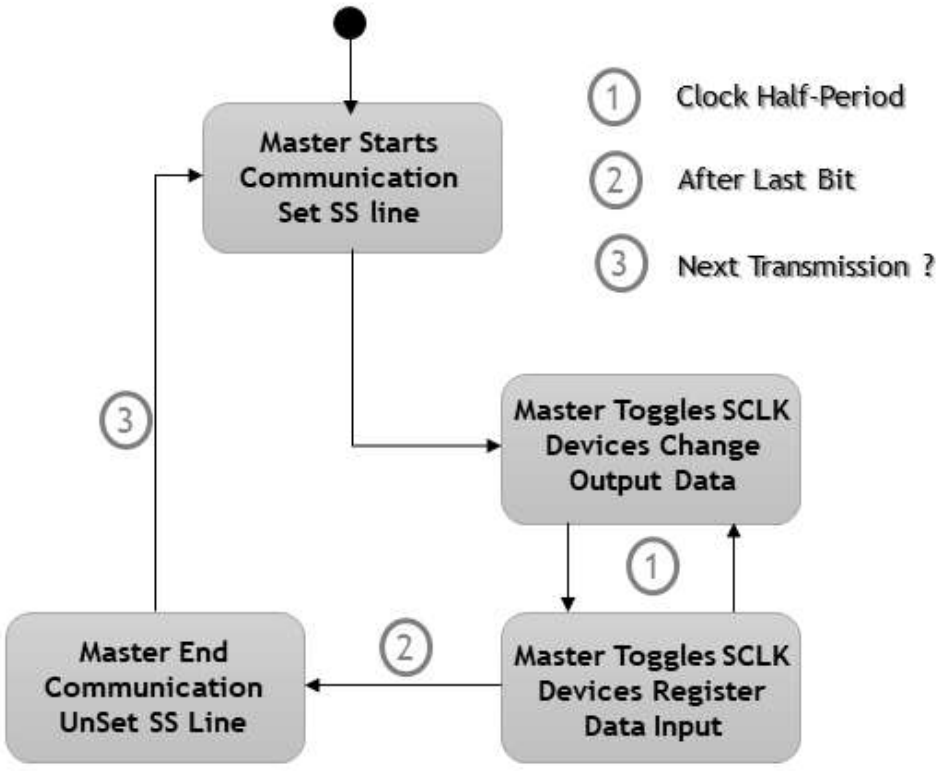

Figure 4.11 - State flow chart of the basic SPI transmission. Adapted from [71].

4.4.1.4 | **SPI Configuration Bits**

The SPI communication clock signal is configurable by two parameters, the polarity (CPOL) and phase (CPHA).

The influence of these configuration bits on the system is as follows:

- For CPOL = 0, the clock signal has zero base logic value.
- With CPHA = 0, information is acquired on the rising edge of the clock signal and is changed during the downward flank.
- With CPHA = 1, the information is read on the downside and modified on the ascending side of the clock sign.
- For CPOL = 1, the clock signal has base logic value one (the inverse of CPOL = 0)
- With CPHA = 0, information is acquired on the downside and changed on the rising flank.
- With CPHA = 1, information is acquired on the rising flank and changed on the downward flank.

4.4.1.5 | SPI Timing considerations

Every SPI compatible hardware devices present timing intervals which define tolerances for the speed, setup and hold times of each signal.

Through Figure 4.12 and Table 4.3, it is possible to observe the SPI timing as well as CPOL and SPI configuration for ADS1194.

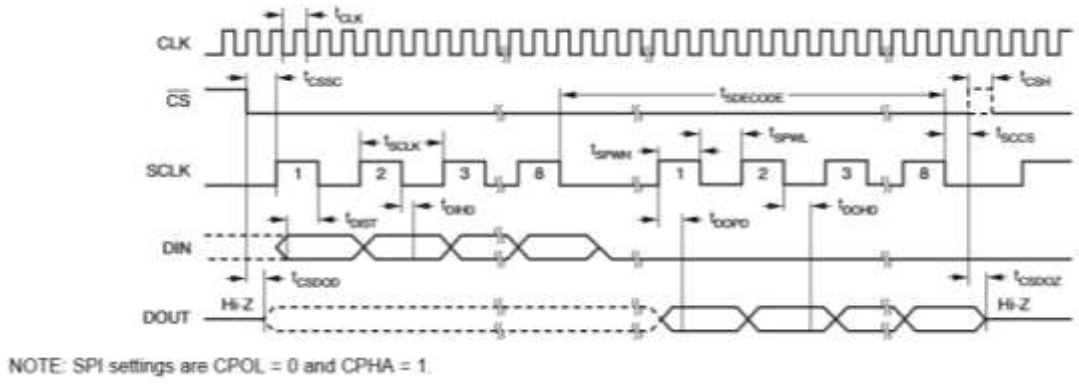

Figure 4.12 - Serial Interface Timing and SPI configuration [85].

Table 4.3 - Timing requirements for ECG2C SPI communications [85].

Parameter	Description	2.7V ≤ DVDD ≤ 3.6V			1.65V ≤ DVDD ≤ 2.0V			Unit
		MIN	TYP	MAX	MIN	TYP	MAX	
t_{CLK}	Master clock period	414			414			ns
t_{CSSC}	$\overline{CS}$ low to first SCLK; setup time	6			17			ns
t_{SCLK}	SCLK period	50			66.6			ns
$t_{SPWH, L}$	SCLK pulse width, high and low	15			25			ns
t_{DIST}	DIN valid to SCLK falling edge; setup time	10			10			ns
t_{DIHD}	Valid DIN after SCLK falling edge; hold time	10			11			ns
t_{DOHD}	SCLK falling edge to invalid DOUT; hold time	10			10			ns
t_{DOPD}	SCLK rising edge to DOUT valid; setup time			17			32	t_{CLKs}
t_{CSH}	$\overline{CS}$ high pulse	2			2			ns
t_{CSDOD}	$\overline{CS}$ ow to DOUT driven	8			20			t_{CLKs}
t_{SCCS}	Eighth SCLK falling edge to $\overline{CS}$ high	4			4			t_{CLKs}
$t_{SDECODE}$	Command decode time	4			4			ns
t_{CSDOZ}	$\overline{CS}$ high to DOUT Hi-Z			10			20	ns
$t_{DISCK2ST}$	DAISY_IN valid to SCLK rising edge; setup time	10			10			ns
$t_{DISCK2HT}$	DAISY_IN valid after SCLK rising edge; hold time	10				10		n

4.5 | Heart rate 4 click

For the oximeter sensor, the Heart rate 4 click (HR4C), represented in Figure 4.13 was chosen. This board carries the MAX30101 high-sensitivity pulse oximeter and HR sensor from Maxim Integrated. Planned to run on either 3.3V or 5V power supply, it connects with the target MCU over Inter-Integrated Circuit (I2C) interface, with additional functionality provided by INT pin on the mikroBUS™ line [86].

Figure 4.13 - Heart rate 4 Click board [86].

4.5.1 | I2C Communication

The I2C communication bus is a two-wire half-duplex serial interface with two bidirectional lines, Serial Data (SDA) and Serial Clock (SCL). To simplify the identification and communication by the master, each device connected to the I2C has a unique 7-bit I2C address. Usually, the upper four bits are fixed and assigned to specific categories of devices. On the other hand, the three lower bits are programmable over hardware address pins, permitting up to eight devices of the same kind to be connected to a single I2C bus [87].

4.5.1.1 | I2C Transfers

By altering the SDA line level from high to low while keeping the SCL clock line high, the master issues a start condition and initiates a transfer. With this, the bus is considered busy, and all devices on the bus become prepared to listen for incoming data. After this, and to configure for the appropriate data transfer, the master sends the 7-bit address and 1-bit for data transfer direction on the bus. All slaves compare the address with their address. When the addresses coincide, the slave produces an ACK (acknowledge) signal.

Then, when this ACK signal is detected by the master, the transmission or reception of data starts. For the transmission of data to a device, the first bit is set onto the SDA line by the master and a clock pulse is generated to transmit the bit through the bus to the slave. On the other hand, to receive data from a device, the master releases the SDA line, permitting the slave to take control of it. Then, and for each bit, the master generates a clock pulse on the SCL, reading the data while the SCL line is high. It is necessary to take into account that while the SCL line is high, the device is not allowed to change the SDA line state [87].

In the end, and after the transmission of the data, the master issues the stop condition by altering the SDA line from low to high while keeping the SCL clock line high. This takes on that the bus is considered free, and another master can initiate a data transfer.

4.5.1.2 | Acknowledge Timing

Since the master controls the clock, a mechanism, known as clock stretching, permits that when not ready, the slave can slow down the bus traffic. During any SCL low phase, a slave might additionally hold down SCL to avert it from rising high again to slow down the SCL clock rate or pause I2C communication.

When the master attempts to make SCL high to complete the current clock pulse, it must verify that it has really gone high. If it is still low, it knows a slave is holding it low and must wait until it goes high before continuing [87].

4.5.1.3 | I2C Pin Description

Serial Data (SDA): This bidirectional pin is used to the transfer of addresses as well as data into and out of the device. Once it is an open-drain terminal, the SDA bus requires a pull-up resistor to VCC. For standard data transfer, SDA is allowed to change merely during SCL low. The changes during SCL high are reserved for indicating the Start and Stop conditions.

Serial Clock (SCL): The purpose of this input is the synchronisation of the data transfer from and to the device [87].

4.6 | Android App

The second main task of this project regards the development of an app to operate within the Android mobile operating system. For this purpose, the Android Studio integrated development environment (IDE) was chosen. This decision was related to the fact that it is a free platform, easy to use and widely recognised for the development of the desired type of applications, being the official IDE for Android applications development.

This system uses a Gradle-based build system, emulator, code templates, and Github integration. Every project in Android Studio has one or more modalities with source code and resource files. These modalities include Android app modules, Library modules, and Google App Engine modules and can be directly downloaded from Google.

4.7 | Firebase

After the Android App, the data should be saved in a cloud service to facilitate the storage and visualisation of the data. For that purpose, several factors were taken into consideration, such as the security of the data, the accessibility in all mobile devices and the compatibility to android and the easy data storage.

With all this in mind, the chosen platform was the firebase, a Google's mobile platform that was created to help the agile app development. This platform provides several tools, like authentication and Realtime database, and have an assistant to connection directly in the android studio tools, the use of this service has proved to be the most appropriate strategy to implement. This system still provides security levels adjusted and the possibility to expand to different services that allow the improvement of the project development.

4.8 | Final Remarks

The system to be developed involves the use of the ECG2C and HR4C interconnected with the Hexiwear platform, to obtain the requested data. This data should then be sent through Bluetooth to an android app, developed in android Studio, allowing the easy visualisation of the data. In the final step, this data should be stored in the firebase Realtime Database, allowing that data can be consulted by the health professional in any place and at any time.

Chapter 5

Project Development

Despite the impossibility of implementing all the intended sensors, the project result is a complete system capable of data acquisition, analysis, visualisation and storage. The three different measurements obtained are the HR, the SpO_2 and the BP. These values can be read in the Hexiwear screen, in the android app or even in the firebase real-time database, as demonstrated below.

5.1 | Data Acquisition

The code for the data acquisition was developed in MBED, an embedded operating system created to facilitate the development of IoT connected products, using Mbed Studio, that provides a well-defined API to develop C++ application [88]. This system was chosen taking into account the Hexiwear development recommendations [47].

5.1.1 | Heart rate and oxygen saturation

To obtain HR and SpO_2 the HR4C oximeter is used. This board uses an I2C communication to connect to Hexiwear. For the definition of the communication properties, we used the MAX30101 integrated pulse oximeter datasheet [89]. This device can support up to three LED

channels of sequential processing (Red, IR, and Green). For reading both HR and SpO_2, it is necessary to activate the R and IR LEDs. When more than one LED is active, a time slot or period exists between active sequential channels.

For the communication between the MAX30101 device and Hexiwear, a MAX30101 library is used [90]. The code flow chart diagram can be seen in Figure 5.1.

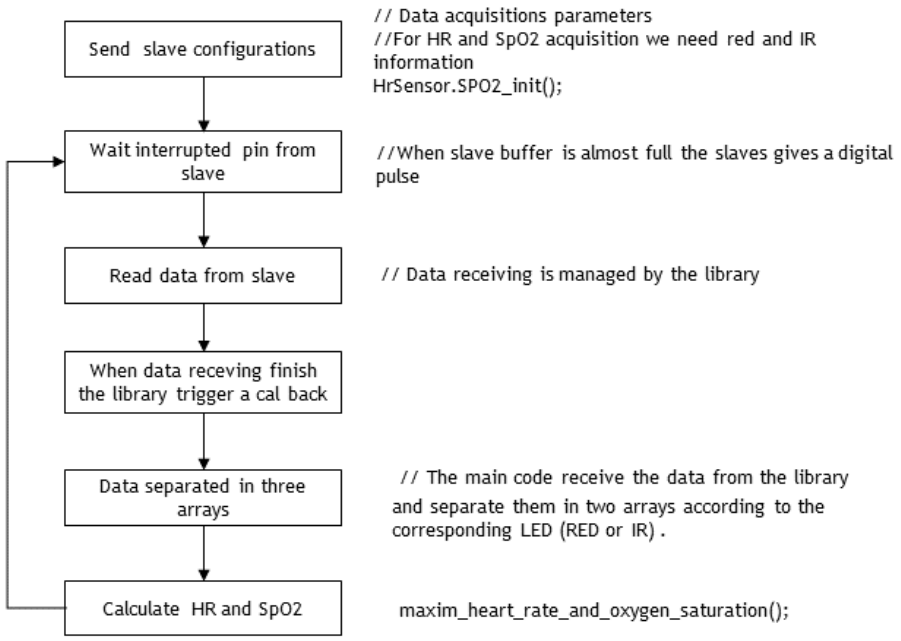

Figure 5.1 - Code flow chart diagram for heart rate and oxygen concentration acquisition.

In the beginning, the Hexiwear (master) send the configurations to the HR4C (slave). After this, the HR4C starts the data acquisitions, and stores it in a buffer. When the buffer is almost full, the slaves give a pulse on a digital pin. This pin is associated with a callback in the master. When the master receives the pulse from the slave, it knows that the buffer is almost full and starts to request data from the slave buffer. This request data is managed by the library. When all the requested data is captured, the library triggers a callback in the main code that separates the data into two arrays, corresponding to the LED from where they originate. Then, in the main loop, the data is filtered, processed, and converted to the desired measurements. With the data from R and IR LEDS, the HR/bpm and SpO_2/% are calculated. More than that, and as can be seen in point 5.2, we can obtain the BP from the signal through the oximeter signal.

Regularly, the oximeter measurements are obtained in a thin part of the patient's body, usually a fingertip or earlobe, or in the case of an infant, across a foot [30]. For this development purposes, data were collected by performing oximeter readers on the finger, in order to facilitate the right connection of the sensor. However, considering the primary purpose of this project, a solution should be achieved in order to obtain measures in the chest.

The SpO_2 values were measured in healthy users, being the obtained values variable between 90% and 100%. This value was compared simultaneously with the CMS50D pulse oximeter, getting a maximum error of about ± 5%. Regarding the assessment of the HR, measures vary between 60 and 82 bpm, with a maximum error of ± 6%. However, further trials are needed.

5.1.2 | ECG Data Acquisition

As stated earlier, ECG monitoring is essential to control cardiac rate and arrhythmic behaviour in patients with HF.

As already mentioned, for ECG recording, ECG2C is used. For testing the SPI communication between ECG2C and the Hexiwear, it was implemented a code for reading the ID of the device. For this, we send a 3 bytes command. The first two bytes correspond to the command to request the slave ID, and the last one is a ‘dummy’ byte to receive the ID from the slave. The signal for this step, represented in Figure 5.2, was obtained using an oscilloscope and shows the three bytes of the serial communication. In the figure, only the SCL and the master out are represented.

Figure 5.2 - Signal obtained in the implementation of the code to read the device ID. The red plot represents the serial clock, and yellow represents the master out (First byte 0b00100000; second byte 0b00000000; third byte 0b00000000).

As can be seen after the diagram represented in Figure 5.3, the code for the data acquisition is similar to that used in the oximeter readings. However, and considering that no library was found that met the requirements, several configuration commands need to be sent first. It was necessary to configure SPI parameters, like frequency, clock polarity and phase. After this, the ECG is reset. Then, the ECG2C configuration is sent, and the channels offset is calculated for each channel. Values are obtained from three channels corresponding to the combinations between the three ECG electrodes (LA RA, LL RA, LL LA) and a fourth channel corresponding to the temperature sensor voltage. After this, the ECG data acquisition starts. The final graph is obtained through the channel LL RA, that is typically used for simple ECG, and built as a function of time.

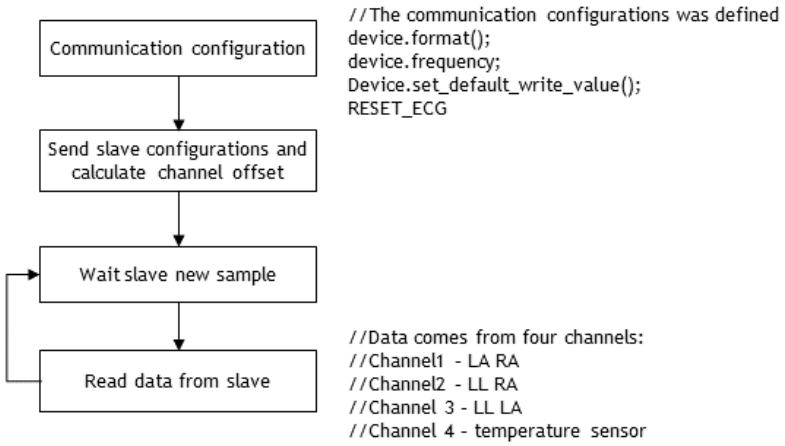

Figure 5.3 - Code flow chart diagram for the acquisition of the electrical activity of the heart and the corresponding time.

For the ECG measurement, three electrodes should be placed on Left Arm (LA), right arm (RA) and Left Leg (LL). However, as can be seen in Figure 5.4, the LL electrode was placed right beneath the heart. This recurrent convention is fundamental given the objective of the project, which is the development of a wearable system.

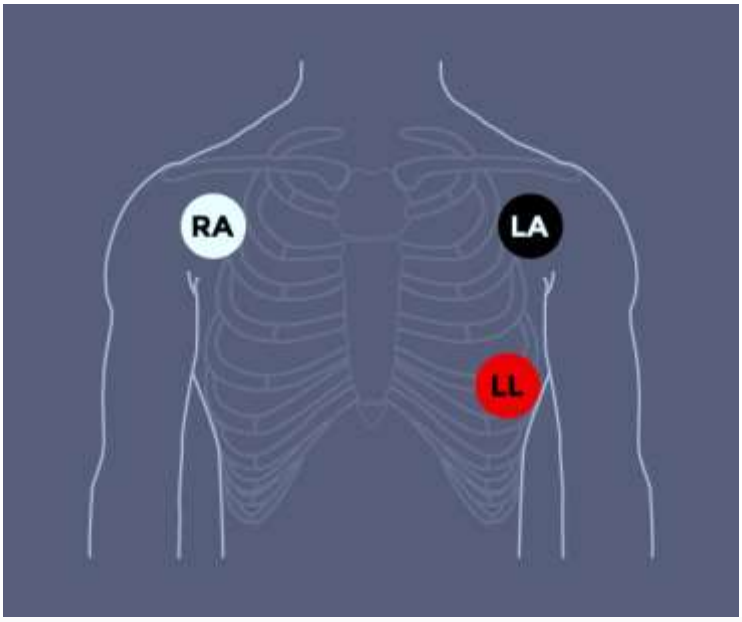

Figure 5.4 - Electrodes placement configuration.

The obtained ECG signal can be seen in Figure 5.5. Due to some hardware problems, the final signal was obtained connecting ECG2C to SP32 microcontroller. Due to the development time and the difficulty of obtaining a sensor for comparison, the data of this sensor were not compared. However, as can be seen from the figure, the obtained wave presents an expected conformation, being possible the visualisation of the several expected peaks in an ECG record.

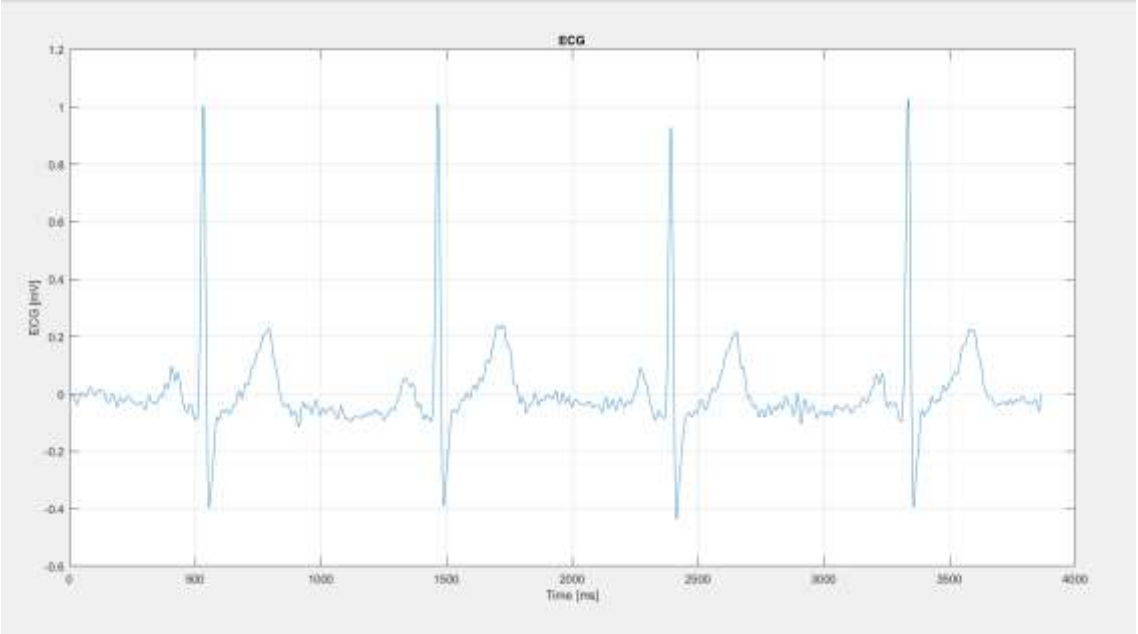

Figure 5.5 – ECG signal obtained with ECG 2 Click connected to SP32.

5.1.3 | Blood Pressure Determination

The continuous monitorization of BP is essential for many clinical situations, including HF. Usually, this measurement is performed using a sphygmomanometer, that consists of an inflatable cuff attached to the measurement device. However, this method of measurement has challenges, such as limited convenience and mobility, the need for frequent measurements, and variability in fitting the cuff [91]. Considering this, in recent years, alternative methods of assessing BP based only on PPG signal or on the simultaneously collected ECG and PPG attracted the interest of many researchers [58, 92].

In this work, the SYS BP was calculated using only the PPG signal, through STT. This signal is passed through a differential filter. First, it is determined the peak of the PPG. Then, defining an arbitrary constant amplitude (150), the STT is obtained. The STT values are obtained in a health patient at rest and after exercise and being compared with BP values obtained with the DBPOWER BP Monitor in the same conditions to obtain a calibration line. This calibration is then applied to the code in order to obtain the final BP measurements (Figure 5.6). The DIA BP has not yet been determined due to reduced sensitivity of STT values.

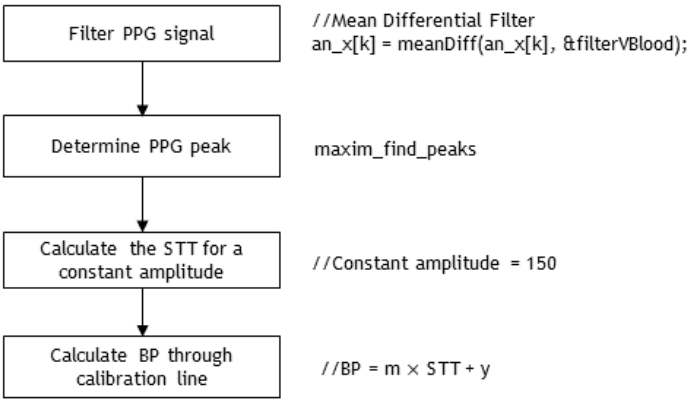

Figure 5.6 - Code flow chart diagram for the blood pressure calculation.

.

The obtained values for one user were compared simultaneously with DBPOWER BP Monitor, and the values show similarities, getting a maximum error of about ± 15.3%. However, the values suffer constant oscillations, and the number of samples obtained is not sufficient to validate the method, and further testing is required.

5.1.4 | Hexiwear program

The complete program that performs the data acquisition and sending is described below. As can be seen in Figure 5.7, After declaring and initialising variables and classes, the main function calls the setups functions of each unity (Bluetooth, screen, oximeter and ECG), responsible for the configurations. Then task for each of the sensors starts, which is responsible for data acquisition (detailed in points 5.1.1 and 5.1.2), and for the Bluetooth communication. After this, a loop changes the LED to the blue colour indicative of Bluetooth availability. The code for the main structure of this program is represented in Appendix A.

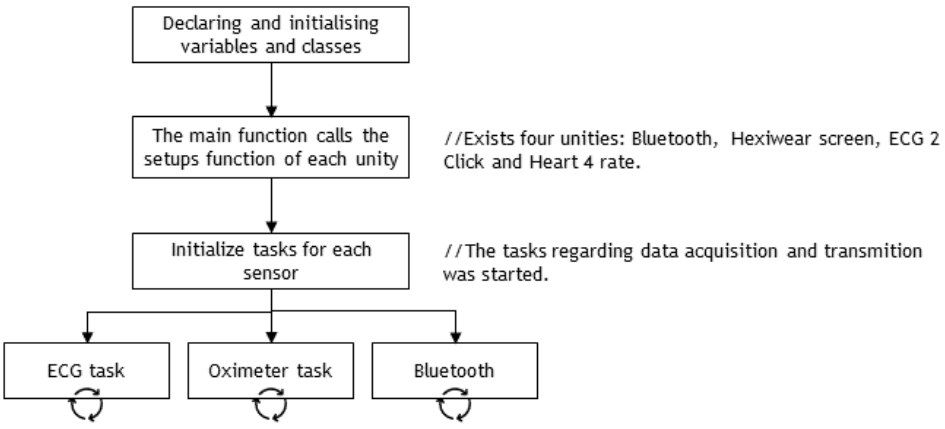

Figure 5.7 - Code flow chart diagram for the Hexiwear program.

5.2 | Android App

As mentioned earlier, an android application, named SafeBeat, and capable of interacting with Hexiwear has been developed. The code flow chart diagram of the applied code can be seen in Figure 5.8. The classes used to create the Mobile Application were divided into six packages, which structure can be seen in Figure 5.9 and are described below.

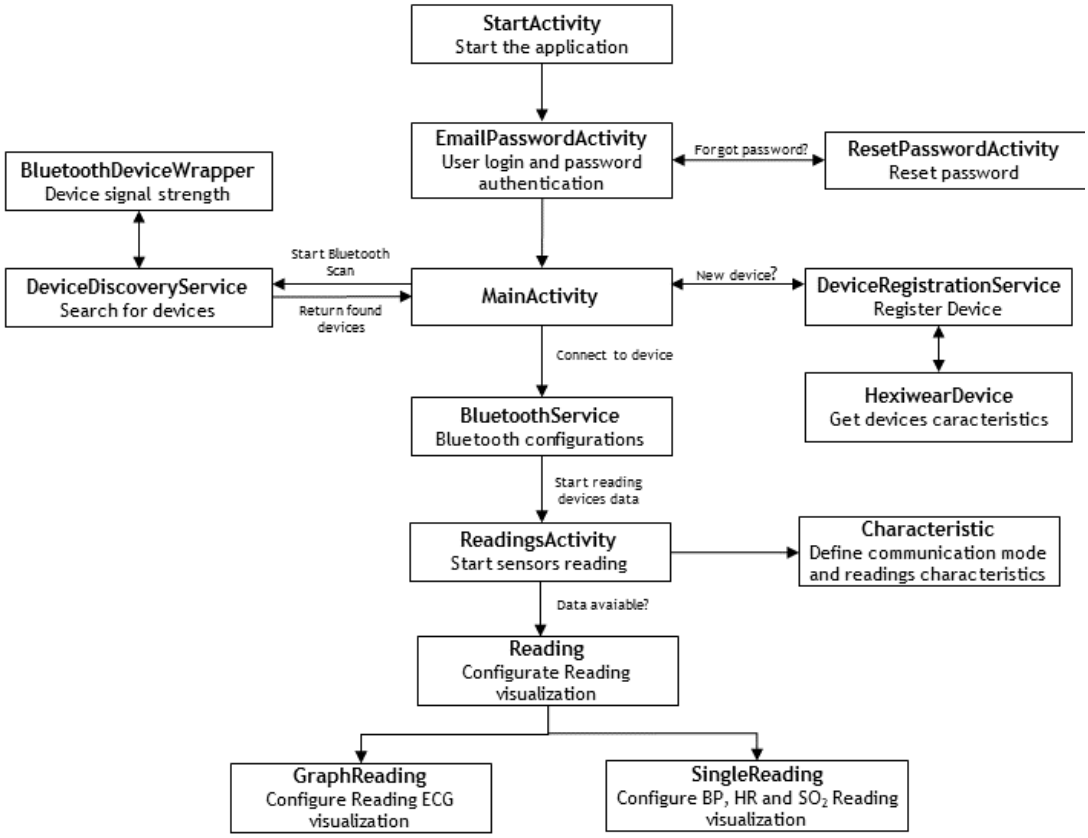

Figure 5.8 - Code flow chart diagram for the android application.

The package activity comprises all the activities directly related to the user. The startActivity is the first activity performed when the application starts and has a button that directs the user to EmailPasswordActivity. It is in this activity that users can register via email and password. The authentication method is connected to the Firebase Database, allowing the

users registration. It is also through this service that it is possible to reset the password, performed by ResetPasswordActivity, which connects with firebase to send a password recovery email. These activities are then linked to MainActivity, which is responsible for controlling the processes necessary for the correct operation of the application until the data acquisition begins, performed by ReadingsActivity's. The MainActivity start the DeviceDiscoveryService in order to start the Bluetooth devices search. The strength of the device's connection is presented by BluetoothDeviceWrapper. At the end of the scan, the DeviceDiscovery service return to the main activity the discovery device. If the selected device is new, the DeviceRegistrationService register them according to the characteristics presented in the HexiwearDevice. Back to the main activity, this starts the connection to the device selected, through BluetoothService. When the device is connected, the ReadingsActivity starts reading data from the devices, which visualization is described in the Reading Class. In turn, the visualisation considering the type of reading is defined in GraphReading (ECG readings) and SingleReadings (BP, HR and SpO_2).

Still, within the app code, the package adapter is responsible for managing the devices available for communication with the application, being HexiwearListAdapter specific to Hexiwear. On the other way, in the model package, the Characteristic class is responsible for defining the specifications of the sensors readings communication, where the id of the Bluetooth feature is defined. The example below defines HeartRate:

```
HEARTRATE (Type.READING, "00002021-0000-1000-8000-00805f9b34fb", "bpm")
```

Still, in the same package, it is performed the definition of the sensor mode. This allows that without changing the application, it is possible to change the displayed data just by changing the send mode. Hexiwear has three predefined modes: SENSOR_TAG, PEDOMETER and HEARTRATE, being the last one used in this project.

The layout of this app consists of a first page where the app starts, followed by a login page where the user has to authenticate using the email and password set to use this service. This login is also connected to the cloud service, being registered which user is using the application, and also allowing the storage of data associated with it. In the case of new users, they are taken to verify the email by clicking on a link received in the email indicated. If forgotten the password, there is also the possibility to receive a way to reset it, again through the email address. After this login, it should be selected the device to connect with, and for the first time, it needs to enter the security code that will appear on the Hexiwear monitor. After this connection, a visualisation page of the collected data is displayed, giving the possibility to monitor values such as HR, SpO_2, BP. To observe the ECG graph, it is necessary to press the ECG button available in the top of the page. The user's flow diagram can be seen in Figure 5.10.

Figure 5.9 – Android App package structure.

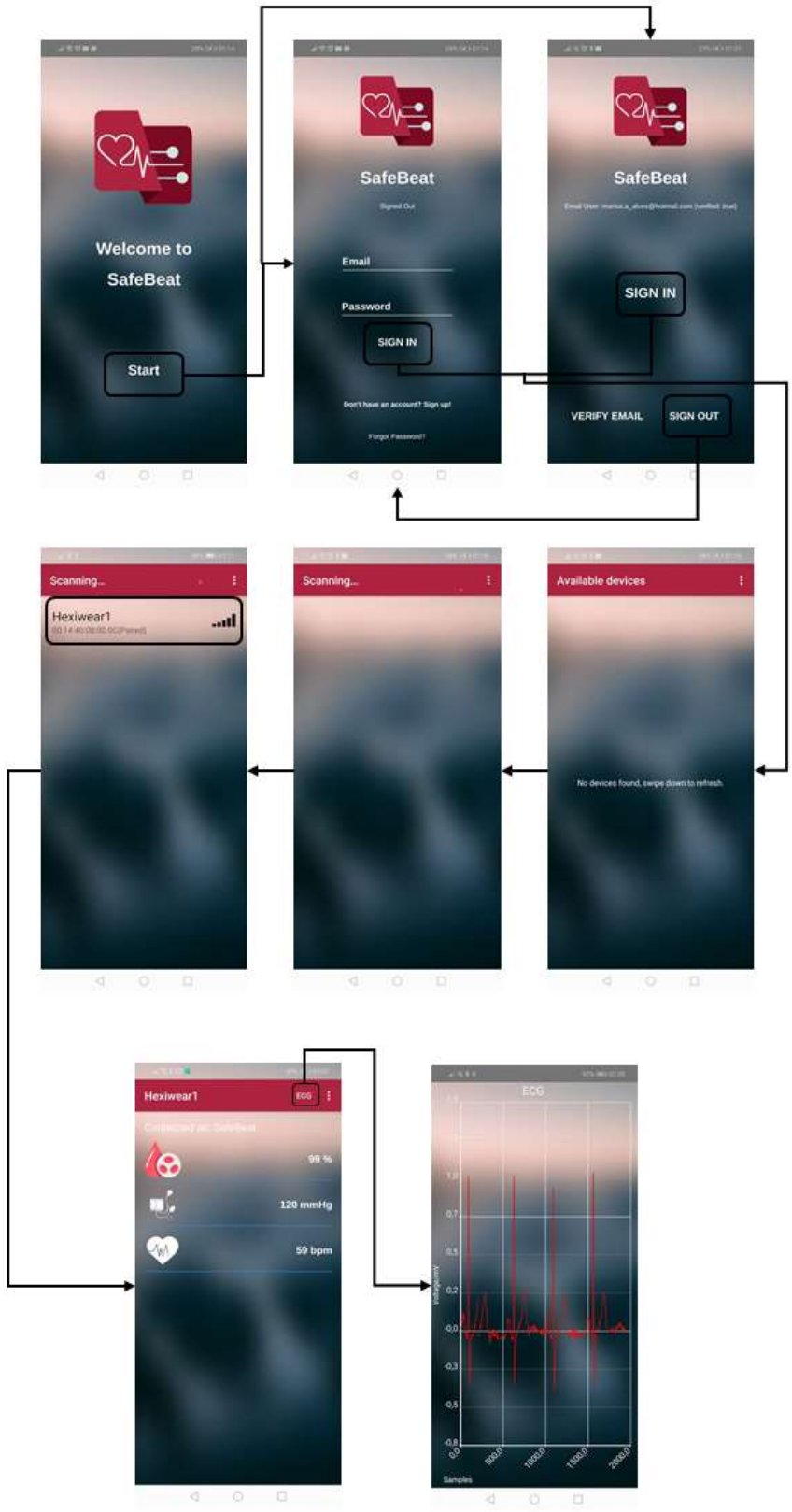

Figure 5.10 - User's flow diagram for the SafeBeat app.

5.3 | Data Storage

As said before, the data was stored in the real-time database using firebase service. This cloud database stays synced to all connected clients in real-time and remains available when the app goes offline. The Data is stored in the JSON tree structure. The read and write access to our database is restricted to authenticated users.

This communication is implemented through the use of AndroidStudio Tools, which provides a guide for this communication and simplify the implementation. The connection of the app to the firebase is implemented before in the user authentication. After adding the Realtime Database to the project, it only needs to initialise the database:

```
FirebaseDatabase database = FirebaseDatabase.getInstance();

DatabaseReference myRef = database.getReference("data");
```

The data recorded corresponding to the HR, SpO_2 and BP values, as can be seen in Figure 5.11.

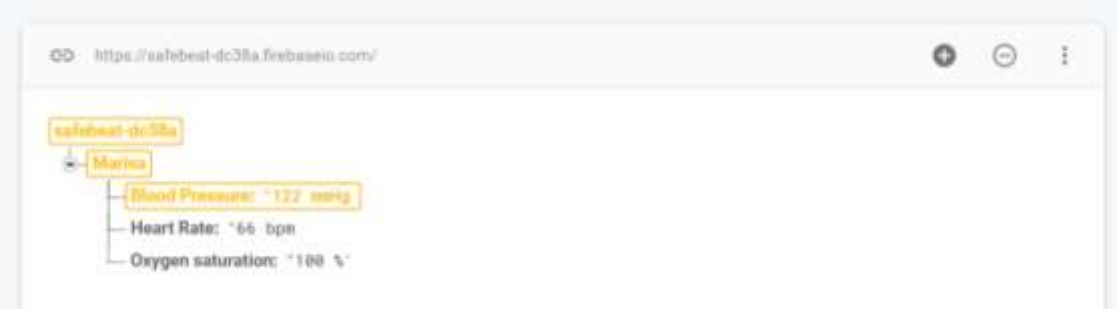

Figure 5.11 - Data visualized in Firebase Realtime Database.

5.4 | Final Remarks

The final system obtained includes the use of two sensors, ECG2C and HR4C, which communicate with Hexiwear through SPI and I2C communication, respectively. These sensors allow obtaining data related to HR, BP, SpO_2 and also to obtain the ECG record. Data visualisation can be done by the user in two ways: through the Hexiwear screen, which only does not allow the visualisation of the ECG graph and also through the SafeBeat app. This app has been specially designed to communicate with Hexiwear for easy and intuitive viewing. Besides, the obtained data are still stored in the firebase Realtime database.

Despite all the difficulties in development, the results presented demonstrate a system that fulfils the initially proposed requirements: it allows the acquisition, visualisation and storage of data of interest to HF. The final result is an autonomous system, capable of obtaining several

values of interest, as HR, SpO_2 and BP. However, it is necessary to obtain more samples of the results obtained, and under different conditions, in order to prove the effectiveness of the implemented methods. It is also necessary to improve the data storage in the database in order to facilitate data consultation and also avoid redundant data.

Chapter 6

Conclusions and Future Work

6.1 | Conclusions

The use of telemedicine in the medical field is not new; however, it is still necessary to go a long way towards achieving infallible systems that meet all the requirements in monitoring the various diseases. Having said that, the creation of a system that can monitor HF patients, accessible by an android app or by the cloud, is, no doubt, an essential evolution for the HF treatment. This system benefits not only patients, as it allows better control of their disease as well as the health system, as the number of hospitalisations is reduced. The complementary treatments are applied more effectively, allowing for a reduction in the costs associated with the treatment of HF.

Depth research has been conducted to detect which biomedical parameters are of interest for monitoring patients with this condition. In the light of this research, for complete and adequate monitoring, values for HR, BP, transthoracic fluid volume, SpO_2 and NaCl concentration in sweat should be obtained. However, taking into account the project time, with all the necessary knowledge to acquire, only two sensors were added, allowing the obtaining of three values: HR, SpO_2 and BP.

A survey of the devices in the market was also performed. Taking into account the results obtained, compared to other systems on the market, the developed system has the advantage of being targeted to the disease in question, being easily adaptable to the remaining sensors and having an intuitive and specific application.

Even though it does not cover all sensors indicated for HF monitoring, the final result includes a fully functional system capable of obtaining HR, blood O_2 levels, BP data and full ECG. Except for the ECG graph, these values can be visualised by the patient in the Hexiwear monitor. Complementing, all data can be seen or in the SafeBeat App, a user-friendly android application specifically designed for this purpose. For healthcare professionals, they can view data in real-time through the cloud service.

6. 2 | Future work

The need to improve the systems used for disease monitoring is evident and will still require much work. Relative to future work that should be implemented in this project, several steps should be followed. First of all, it is necessary to implement the remaining necessary sensors: the chemical sensor for determination of sweat NaCl and the sensor of electrical bioimpedance. With these implementations, all the intended measurements can be obtained. It is necessary to test and improve the BP detention method, in order to prove that the method used is a viable method for measurement. After this, it was necessary to convert the system to constant measurements. Data storage should also be optimised by keeping only a daily summary of results, and then sending a monthly report to the responsible health professional, highlighting the minor abnormalities. The alert levels available should also be improved and direct contact with the healthcare professional when symptoms so require.

For conclusion, it is necessary to convert the project into a wearable system capable of obtaining data as efficiently as possible.

Appendix A

```
1.  /*********************************************************************
2.  *A WEARABLE SYSTEM FOR REMOTE CARDIORESPIRATORY FITNESS MONITORING
3.  *MARISA ALVES    | P. DR. JOSE MACHADO DA SILVA
4.  *********************************************************************/
5.
6.  #include "mbed.h"
7.
8.  #define LED_ON      0
9.  #define LED_OFF     1
10.
11. Serial pc(USBTX, USBRX,9600); // pc interface
12.
13. int32_t mean(int32_t *arr, uint16_t size){
14.     int32_t meanv = 0;
15.     for (int i = 0; i<size;i++) meanv+=arr[i];
16.     return meanv/size;
17. }
18.
19. ////////////////////////////////////////////////////////////////////////
20. ////////////////////////////// Settings for OLED Class ////////////////////////
21. ////////////////////////////////////////////////////////////////////////
22.
23. #include "Hexi_OLED_SSD1351.h"
24. #include "OLED_types.h"
25. #include "OpenSans_Font.h"
26.
27. /* Instantiate the SSD1351 OLED Driver */
28. SSD1351 oled(PTB22,PTB21,PTC13,PTB20,PTE6, PTD15); /* (MOSI,SCLK,POWER,CS,RST,
    DC) */
29.  /* Text Buffer */
30. char text[20];
31. oled_text_properties_t textProperties = {0};
32.
33.
34. ////////////////////////////////////////////////////////////////////////
35. ////////////////////////// Settings for HeartRate4Clcik ////////////////////
36. ////////////////////////////////////////////////////////////////////////
37.
38. #include "MAX30101.h"
39. #include "HeartRate4Click/MAX30101_Defines.h"
40. #include "HeartRate4Click/spo2_algorithm.h"
41.
```

```
42. #define FIFO_WATERLEVEL_MARK 0x07 //25 Samples Note: 0x00 is 32 samples, 0x0F
    is 17 samples
43. #define SAMPLE_AVG           MAX30105_SAMPLEAVG_4    //Options: 1, 2, 4, 8, 16
    , 32
44. #define SAMPLE_RATE          MAX30100_SAMPRATE_100HZ //Options: 50, 100, 200,
    400, 800, 1000, 1600, 3200
45. #define PULSE_WIDTH          MAX30100_SPC_PW_400US_16BITS //Options: 69, 118,
    215, 411
46. #define RED_LED_CURRENT      60  //Options: 0=Off to 255=50mA
47. /// Buffer size to hold Recv Data.
48. #define BUFFER_LENGTH 100 //4 seconds of data
49.
50. //Initializa HeartRate4Clcik Class
51. MAX30101 HrSensor(PTD9, PTD8, MAX30101_I2C_SLAVE_ADDR);  // SDA, SCL, i2c 7-
    bit address
52. InterruptIn max30101_Interrupt(PTB13);
53.
54. //Functions Prototypes
55. void hearRateTask(void);
56.
57. //Variables Defenitions
58. uint32_t oxiBuffer1RED[BUFFER_LENGTH];
59. uint32_t oxiBuffer2IR[BUFFER_LENGTH];
60. uint32_t oxiBuffer3GREEN[BUFFER_LENGTH];
61. int oxiIndex = 0;
62. char data_trigger = 0;
63. char int_trigger = 0;
64. int32_t iravgreg = 0;
65. int nSamples = 0;
66. uint8_t validSamples = 0;
67.
68. /*Create a Thread to handle reciving data*/
69. Thread heartRateRxThread(osPriorityNormal,
70.                          OS_STACK_SIZE,
71.                          NULL, "Heart Rate Thread!");
72.
73. /**************************Call Back Functions*****************************
    */
74. //@brief Creates a packet that will be streamed via USB Serial
75. //@brief the packet created will be inserted into a fifo to be streamed at a l
    ater time
76. //@param id Streaming ID
77. //@param buffer Pointer to a uint32 array that contains the data to include in
     the packet
78. //@param number Number of elements in the buffer
79. //
80. void StreamPacketUint32_ex(uint32_t id, uint32_t *buffer, uint32_t number) {
81.     int i;
82.     int slotIdx = 1;
83.     if (id == MAX30101_OXIMETER_DATA + 3) {
84.         nSamples = number/3;
85.         memmove(&oxiBuffer1RED, &oxiBuffer1RED[nSamples], sizeof(oxiBuffer1RED
    )-(nSamples*sizeof(oxiBuffer1RED[1])));
86.         memmove(&oxiBuffer2IR, &oxiBuffer2IR[nSamples], sizeof(oxiBuffer2IR)-
    (nSamples*sizeof(oxiBuffer2IR[1])));
87.         memmove(&oxiBuffer3GREEN, &oxiBuffer3GREEN[nSamples], sizeof(oxiBuffer
    3GREEN)-(nSamples*sizeof(oxiBuffer3GREEN[1])));
88.
89.         oxiIndex = 1;
90.         for (i = 0; i < number; i++) {
91.             switch(slotIdx){
92.                 case 1:
93.                     //pc.printf("RED: %d\n\r",buffer[i]);
94.                     //pc.printf("%d\n\r",buffer[i]);
95.                     oxiBuffer1RED[BUFFER_LENGTH-oxiIndex] = buffer[i];
```

```
96.                     slotIdx++;
97.                     break;
98.                 case 2:
99.                     //pc.printf("IR: %d\n\r",buffer[i]);
100.                            oxiBuffer2IR[BUFFER_LENGTH-oxiIndex] = buffer[i];
101.                            slotIdx++;
102.                            break;
103.                        case 3:
104.                            //pc.printf("GREEN: %d\n\r",buffer[i]);
105.                            oxiBuffer3GREEN[BUFFER_LENGTH-
    oxiIndex] = buffer[i];
106.                            oxiIndex++;
107.                            slotIdx = 1;
108.                            break;
109.                    }
110.                }
111.                data_trigger = 1;
112.            }else if (id == MAX30101_OXIMETER_DATA + 2) {
113.                nSamples = number/2;
114.                memmove(&oxiBuffer1RED, &oxiBuffer1RED[nSamples], sizeof(oxiBuf
    fer1RED)-(nSamples*sizeof(oxiBuffer1RED[1])));
115.                memmove(&oxiBuffer2IR, &oxiBuffer2IR[nSamples], sizeof(oxiBuffe
    r2IR)-(nSamples*sizeof(oxiBuffer2IR[1])));
116.
117.                oxiIndex = 1;
118.                for (i = 0; i < number; i++) {
119.                    switch(slotIdx){
120.                        case 1:
121.                            //pc.printf("RED: %d\n\r",buffer[i]);
122.                            oxiBuffer1RED[BUFFER_LENGTH-
    oxiIndex] = buffer[i];
123.                            slotIdx++;
124.                            break;
125.                        case 2:
126.                            //pc.printf("%d\n\r",buffer[i]);
127.                            oxiBuffer2IR[BUFFER_LENGTH-oxiIndex] = buffer[i];
128.                            oxiIndex++;
129.                            slotIdx = 1;
130.                            break;
131.                    }
132.                }
133.                data_trigger = 1;
134.            }
135.        }
136.
137.        void int_trigCallBack(){
138.            int_trigger = 1;
139.        }
140.        /***********************End of Call Back Functions*******************/
141.
142.
143.        ////////////////////////////////////////////////////////////////////////
144.        ////////////////////////////// Settings for ECG2Click //////////////////
145.        ////////////////////////////////////////////////////////////////////////
146.
147.        #include "Ecg2Click/ecg2_hal.h"
148.        #include "Ecg2Click/ecg2_hw.h"
149.
150.        //Slot 3
151.        #define PAC_ PTB6
152.        #define RESET_EGC_ PTB10
153.        #define CS_ECG_ PTC2
154.        #define PWDN_ PTA4
155.        #define DRDY_ PTB7
156.        #define SIN PTC6
```

```
157.        #define SOUT PTC7
158.        #define CLK PTC5
159.
160.        //Slot 1
161.        #if 0
162.        #define PAC_ PTB2
163.        #define RESET_EGC_ PTB11
164.        #define CS_ECG_ PTC4
165.        #define PWDN_ PTA1
166.        #define DRDY_ PTB13
167.        #define SIN PTC6
168.        #define SOUT PTC7
169.        #define CLK PTC5
170.        #endif
171.
172.        static const int spiClk = 4000000;// 4 MHz
173.        // specific ADC constants
174.        const int num_bytes_sample = 19;        // number of bytes in ADS1194 s
    ample in data continuous mode
175.        const double channel_gain = 20.00;      // amplifier gain
176.        const double refV = 2400.00;            // reference voltage in millivo
    lts
177.
178.        // variable for ADC
179.        unsigned char ecg_data_sample[num_bytes_sample];  // one sample data fr
    om ADS1194
180.        double channel1_voltage; // channel 1 millivolts
181.        double channel2_voltage; // channel 2 millivolts
182.        double channel3_voltage; // channel 3 millivolts
183.        double channel4_voltage; // channel 4 millivolts
184.        double channel1_voltage_offset; // channel 1 offset millivolts
185.        double channel2_voltage_offset; // channel 2 offset millivolts
186.        double channel3_voltage_offset; // channel 3 offset millivolts
187.        double channel4_voltage_offset; // channel 4 offset millivolts
188.
189.        double time_value = 0.0;
190.
191.        gpio_t gpio;
192.
193.        DigitalOut PWDN(PWDN_);
194.        DigitalOut RESET_EGC(RESET_EGC_);
195.        DigitalIn DRDY(DRDY_);
196.        DigitalIn PAC(PAC_);
197.        DigitalOut CS_ECG(CS_ECG_,1);
198.
199.        SPI device(SIN,SOUT,CLK);
200.
201.        Thread ecgThread(osPriorityNormal,
202.                    OS_STACK_SIZE,
203.                    NULL, "Ecg Rx Loop");
204.
205.        //Functions Prototypes
206.        void ecgTask(void);
207.
208.        /*****************************************************************
209.        * Function Definitions
210.        *****************************************************************/
211.        uint8_t vspiCommand(uint8_t data)
212.        {
213.            uint8_t responce;
214.            responce = device.write(data);
215.            return responce;
216.        }
217.
218.        void ecg2_hal_cs( uint8_t logic )
```

```
219.        {
220.            if (logic == 1) {
221.                CS_ECG.write(1);
222.                //wait_us(10);
223.                device.unlock();
224.            } else {
225.                device.lock();
226.                //wait_us(10);
227.                CS_ECG.write(0);
228.            }
229.        }
230.
231.        void ecg2_hal_rts ( uint8_t logic )
232.        {
233.            if (logic)
234.                RESET_EGC = 1;
235.            else
236.                RESET_EGC = 0;
237.        }
238.
239.        /**
240.          @brief calculate_ecg_channel
241.          - Calculates the specific channel voltage in milivolts
242.          @param buffer
243.          - Buffer with the data samples from the ECG2 click
244.          @param index
245.          - Index of the buffer where the value is stored
246.          @param ref
247.          - Reference voltage in milivolts
248.          @param gain
249.          - Channel gain
250.          @param offset_voltage
251.          - Channel voltage offset
252.          @return
253.          - channel voltage in milivolts
254.        */
255.        double calculate_ecg_channel( unsigned char *buffer, unsigned short ind
    ex, double ref, double gain, double offset_voltage )
256.        {
257.          int adc_value = 0;
258.          adc_value = 0;
259.          adc_value = buffer[index];
260.          adc_value <<= 8;
261.          adc_value |= buffer[index + 1];
262.          return ( ((double)adc_value * (ref / (32768 - 1))) / gain ) - offset_
    voltage;
263.        }
264.        /*************** END OF FUNCTIONS ***********************************/
265.
266.
267.        ////////////////////////////////////////////////////////////////////////
268.        ////////////////////////// Settings for Bluetooth Class ///////////////
269.        ////////////////////////////////////////////////////////////////////////
270.
271.        #include "Hexi_KW40Z.h"
272.
273.        //Variables Defenitions
274.        DigitalOut redLed(LED1,1);
275.        DigitalOut greenLed(LED2,1);
276.        DigitalOut blueLed(LED3,1);
277.        DigitalOut haptic(PTB9);
278.
279.        //Fucntions Prototypes
280.        void StartHaptic(void);
281.        void StopHaptic(void const *n);
```

```
282.        void txTask(void);
283.
284.        /* Instantiate the Hexi KW40Z Driver (UART TX, UART RX) */
285.        KW40Z kw40z_device(PTE24, PTE25);
286.
287.        /*Create a Thread to handle sending BLE Sensor Data */
288.        Thread txThread(osPriorityNormal,
289.                        OS_STACK_SIZE,
290.                        NULL, "Bluetooth Tx Loop");
291.
292.        /***************************Call Back Functions*********************/
293.        void ButtonRight(void)
294.        {
295.            //StartHaptic();
296.            kw40z_device.ToggleAdvertisementMode();
297.        }
298.
299.
300.        void PassKey(void)
301.        {
302.            /* Display Bond Pass Key in a 95px by 18px textbox at x=0,y=40 */
303.            sprintf(text,"%d", kw40z_device.GetPassKey());
304.            oled.Label((uint8_t *)text,5,80);
305.        }
306.        /***********************End of Call Back Functions******************
307.
308.
309.        //Variables to Hold Sensor Processed Data
310.        uint8_t battery = 100;
311.        uint16_t xAcc = 0;
312.        uint16_t yAcc = 5000;
313.        uint16_t zAcc = 10000;
314.        int32_t heartrate = 0;
315.        int32_t SpO2 = 0;
316.        uint16_t ecgVoltage = 0;
317.        int32_t bloodPresure = 0;
318.
319.        int8_t validSPo2;
320.        int8_t validHeartRate;
321.        int8_t bloodPresureValid;
322.
323.
324.        void setupBLE(){
325.            /* Register callbacks to application functions */
326.            kw40z_device.attach_buttonLeft(&ButtonRight);
327.            kw40z_device.attach_buttonRight(&ButtonRight);
328.            kw40z_device.attach_passkey(&PassKey);
329.        }
330.
331.        void setupOLED(){
332.            /* Turn on the backlight of the OLED Display */
333.            oled.DimScreenON();
334.
335.            /* Fills the screen with solid black */
336.            oled.FillScreen(COLOR_BLACK);
337.
338.            /* Get OLED Class Default Text Properties */
339.            oled.GetTextProperties(&textProperties);
340.
341.            /* Change font color to Blue */
342.            textProperties.fontColor   = COLOR_BLUE;
343.            oled.SetTextProperties(&textProperties);
344.
345.            /* Display Label at x=22,y=80 */
346.            strcpy((char *) text,"Tap Below");
```

```
347.            oled.Label((uint8_t *)text,22,80);
348.
349.            /* Change font color to white */
350.            textProperties.fontColor   = COLOR_WHITE;
351.            textProperties.alignParam = OLED_TEXT_ALIGN_CENTER;
352.            oled.SetTextProperties(&textProperties);
353.        }
354.
355.        void setupHeartRate4Clcik(){
356.
357.            memset(&oxiBuffer1RED,0,sizeof(oxiBuffer1RED));
358.            memset(&oxiBuffer2IR,0,sizeof(oxiBuffer2IR));
359.            memset(&oxiBuffer3GREEN,0,sizeof(oxiBuffer3GREEN));
360.
361.            // MAX30101 initialize interrupt
362.            HrSensor.onDataAvailable(&StreamPacketUint32_ex);
363.            //max30101_Interrupt.fall(&MAX30101::MidIntHandler);
364.            max30101_Interrupt.fall(&int_trigCallBack);
365.            max30101_Interrupt.enable_irq();
366.
367.            #if 0
368.            HrSensor.Multimode_init(FIFO_WATERLEVEL_MARK, SAMPLE_AVG,
369.                                    SAMPLE_RATE, PULSE_WIDTH,
370.                                    RED_LED_CURRENT, RED_LED_CURRENT,
371.                                    RED_LED_CURRENT, 0b0001, 0b0010,
372.                                    0b0011, 0b0000);
373.            #endif
374.            #if 0
375.            HrSensor.Multimode_init(FIFO_WATERLEVEL_MARK, SAMPLE_AVG,
376.                                    SAMPLE_RATE, PULSE_WIDTH,
377.                                    RED_LED_CURRENT, RED_LED_CURRENT,
378.                                    RED_LED_CURRENT, 0b0001, 0b0010,
379.                                    0b0000, 0b0000);
380.            #endif
381.            #if 1
382.            HrSensor.SpO2mode_init(FIFO_WATERLEVEL_MARK,
383.                                    SAMPLE_AVG, SAMPLE_RATE,
384.                                    PULSE_WIDTH, RED_LED_CURRENT, RED_LED_CURRENT);
385.            #endif
386.            sprintf(text,"SpO2: ");
387.            oled.Label((uint8_t *)text,10,25);
388.            sprintf(text,"HR: ");
389.            oled.Label((uint8_t *)text,10,5);
390.            sprintf(text,"BP: ");
391.            oled.Label((uint8_t *)text,10,45);
392.        }
393.
394.
395.        void setupEcg()
396.        {
397.            // init SPI
398.            //pin_mode(SIN, PullUp);
399.            device.format(8,1);
400.            device.frequency(spiClk);
401.            device.set_default_write_value(0x00);
402.
403.            wait_ms(10);
404.
405.            PWDN = 1;
406.            RESET_EGC = 1;
407.            wait(1);
408.            // issue RESET pulse
409.            RESET_EGC = 0;
410.            wait_ms(1000);
```

```
411.            RESET_EGC = 1;
412.
413.        }
414.        void configureEcg()
415.        {
416.
417.            wait_ms(1);
418.            ecg2_hal_send_command(SDATAC_COMMAND);
419.            wait_ms(1);
420.            ecg2_hal_send_command(RESET_COMMAND);
421.            wait_ms(1);
422.            ecg2_hal_send_command(STOP_COMMAND);
423.            wait_ms(1);
424.            uint8_t tempbuff;
425.            ecg2_hal_read_bytes(ID_REG, &tempbuff, 1);
426.            pc.printf("ID: %d!\n",tempbuff);
427.            wait_ms(10);
428.
429.            uint8_t tempctr;
430.            ecg2_oscillator_clock_enable(true);
431.            ecg2_set_output_data_rate(SPS_125);
432.            //no test signal, default value
433.            ecg2_set_test_source(TEST_SOURCE_EXTERNAL);
434.
435.            // RDL internal and enabled, reference voltage is 2.4V, RLD signal
    source is internal
436.            ecg2_power_down_reference_buffer_enable(true);
437.            ecg2_set_reference_voltage(VREF_2_4V);
438.            ecg2_rld_measurement_enable(true);
439.            ecg2_rldref_source_select(RLDEF_SIGNAL_INTERNAL);
440.            ecg2_rld_buffer_enable(true);
441.            // lead-
    off is in DC mode and using pull up and down resistors, comparator thresholds
    are set to 70% and 30%
442.            ecg2_lead_off_comparator_threshold_set(POSITIVE_70);
443.            ecg2_vlead_off_enable(false);
444.            ecg2_ilead_off_magnitude_set(NA_4);
445.            ecg2_flead_off_frequency_set(3);
446.
447.            // channel is on and gain is 0, input shorted for offset measuremen
    ts
448.            ecg2_configure_channel(1, false, 0, 1);
449.
450.            // channel is on and gain is 0, input shorted for offset measuremen
    ts
451.            ecg2_configure_channel(2, false, 0, 1);
452.
453.            // channel is on and gain is 0, input shorted for offset measuremen
    ts
454.            ecg2_configure_channel(3, false, 0, 1);
455.            // channel is on and gain is 0, input shorted for offset measuremen
    ts
456.            ecg2_configure_channel(4, false, 0, 1);
457.            // channel 1 is used for RDL
458.            ecg2_right_leg_positive_drive_set(2);
459.            // channel 1 is used for RDL
460.            ecg2_right_leg_negative_drive_set(2);
461.            // channel 3P uses pull-up resistor to detect LL lead-
    off, channel 1P uses pull-up resistor to detect LA lead-off,
462.            ecg2_lead_off_positive_channel_select(5);
463.            // channel 2N uses pull-down resistor to detect RA lead-off
464.            ecg2_lead_off_negative_channel_select(2);
465.            // no flip
466.            ecg2_lead_off_current_direction_select(0);
```

```
467.            // continuous conversion mode, WCT not connected to RLD, LOFF compa
    rators enabled
468.            ecg2_lead_off_comparator_enable(true);
469.            // activate conversion to read and calculate offset
470.
471.            ecg2_hal_send_command(START_COMMAND); // send START command
472.            wait_ms(1);
473.            ecg2_hal_send_command(RDATA_COMMAND); // enable read data once
474.            //wait_ms(1);
475.            while (DRDY) {} // wait_ms for ADS1194 device to prepare output dat
    a.
476.            ecg2_hal_cs(0);
477.            wait_us(10);
478.            //for (tempctr = 0; tempctr < num_bytes_sample; tempctr++) { ecg_da
    ta_sample[tempctr] = device.write(0x00); } // read ADS1194 output data, one sa
    mple
479.            for (tempctr = 0; tempctr < num_bytes_sample; tempctr++) {
480.                ecg_data_sample[tempctr] = vspiCommand(0x00);    // read ADS119
    4 output data, one sample
481.            }
482.            // calculate offset
483.            // offset voltage LA RA
484.            channel1_voltage_offset = calculate_ecg_channel( ecg_data_sample, 3
    , refV, channel_gain, 0 );
485.            // offset voltage LL RA
486.            channel2_voltage_offset = calculate_ecg_channel( ecg_data_sample, 5
    , refV, channel_gain, 0 );
487.            // offset voltage LL LA
488.            channel3_voltage_offset = calculate_ecg_channel( ecg_data_sample, 7
    , refV, channel_gain, 0 );
489.            // offset voltage
490.            channel4_voltage_offset = calculate_ecg_channel( ecg_data_sample, 9
    , refV, channel_gain, 0 );
491.            wait_us(10);
492.            ecg2_hal_cs(1);
493.            wait_ms(1);
494.
495.            // stop conversion
496.            ecg2_hal_send_command(STOP_COMMAND); // send STOP command
497.            wait_ms(1);
498.            ecg2_hal_send_command(SDATAC_COMMAND); // SDATAC mode
499.            // activate conversion
500.            // channel 1 settings register
501.            // channel is on and gain is 12, normal electrode input
502.            ecg2_configure_channel(1, false, 6, 6);
503.            // channel 2 settings register
504.            // channel is on and gain is 12, normal electrode input
505.            ecg2_configure_channel(2, false, 6, 0);
506.            // channel 3 settings register
507.            // channel is on and gain is 12, normal electrode input
508.            ecg2_configure_channel(3, false, 6, 0);
509.            // channel 4 settings register
510.            // channel is on and gain is 12, temperature sensor
511.            ecg2_configure_channel(4, false, 6, 4);
512.            ecg2_hal_send_command(START_COMMAND); // send START command
513.            wait_ms(1);
514.            ecg2_hal_send_command(RDATAC_COMMAND); // enable read data in conti
    nuous mode
515.
516.            wait_ms(1);
517.        }
518.
519.        /*******************************Main*******************************/
520.
521.        int main()
```

```
522.        {
523.            /**************Setup**************/
524.            setupBLE();
525.            setupOLED();
526.            setupHeartRate4Clcik();
527.            setupEcg();
528.
529.            /*Start HeartRate4Click Cycle*/
530.            heartRateRxThread.start(hearRateTask);
531.
532.            /*Start ECG2Click Cycle*/
533.            ecgThread.start(ecgTask);
534.
535.            /*Start transmitting Sensor Data */
536.            txThread.start(txTask);
537.
538.            /**************Main Loop**************/
539.            while (true)
540.            {
541.                blueLed = !kw40z_device.GetAdvertisementMode(); /*Indicate BLE
    Advertisment Mode*/
542.                ThisThread::sleep_for(50);
543.            }
544.        }
545.
546.        /*****************************End of Main****************************/
547.
548.
549.        /* txTask() transmits the sensor data */
550.        void txTask(void){
551.
552.           while (true)
553.           {
554.                /*Notify Hexiwear App that it is running Sensor Tag mode*/
555.                kw40z_device.SendSetApplicationMode(GUI_CURRENT_APP_HEART_RATE)
    ;
556.
557.                /*Send Battery Level */
558.                //kw40z_device.SendBatteryLevel(battery);
559.
560.                /*Send Accel Data. */
561.                //kw40z_device.SendAccel(zAcc,xAcc,yAcc);
562.
563.                    if(heartrate < 255 && heartrate >= 0) {
564.                        kw40z_device.SendHeartRate(heartrate);
565.                    }else{
566.                        kw40z_device.SendHeartRate(0);
567.                    }
568.
569.                /*Send SPO2*/
570.                    if (SpO2 < 255 && SpO2 >= 0){
571.                        kw40z_device.SendSpO2(SpO2);
572.                    }else{
573.                        kw40z_device.SendSpO2(0);
574.                    }
575.
576.                /*Send Blood Pressure*/
577.                    if (bloodPresure < 255 && bloodPresure >= 0){
578.                        kw40z_device.SendBP(bloodPresure);
579.                    }else{
580.                        kw40z_device.SendBP(0);
581.                    }
582.
583.                /*Send ECG*/
584.                    kw40z_device.SendEcG(channel2_voltage);
```

```
585.
586.                 ThisThread::sleep_for(1000);
587.             }
588.         }
589.
590.         void hearRateTask(){
591.             int32_t heartrateArr[6];
592.             int32_t bloodPresArr[6];
593.             uint8_t first = 0;
594.             while (true)
595.             {
596.                 if(int_trigger == 1)
597.                 {
598.                     HrSensor.int_handler();
599.                     int_trigger = 0;
600.                 }
601.
602.
603.                 if(data_trigger == 1)
604.                 {
605.                     data_trigger =0;
606.
607.                     //Check finger present
608.                     textProperties.fontColor = COLOR_RED;
609.                     oled.SetTextProperties(&textProperties);
610.                     if (oxiBuffer1RED[BUFFER_LENGTH-1] < 500){
611.                         sprintf(text,"No Finger!!");
612.                         validSamples = 0;
613.                     }else{
614.                        if (validSamples<4){
615.                         validSamples ++;
616.                         sprintf(text,"%d",4-validSamples);
617.                        } else{
618.                         sprintf(text,"");
619.                        }               }
620.                     textProperties.fontColor    = COLOR_WHITE;
621.                     oled.SetTextProperties(&textProperties);
622.
623.                     //4 samples after finger is placed
624.                     validHeartRate = 0;
625.                     validSPo2 = 0;
626.                     bloodPresureValid = 0;
627.                     if (validSamples >= 4){
628.                         maxim_heart_rate_and_oxygen_saturation(oxiBuffer2IR, BU
    FFER_LENGTH, oxiBuffer1RED, &bloodPresure, &bloodPresureValid, &SpO2, &validSP
    o2, &heartrate, &validHeartRate);
629.                     }
630.                     if (validSPo2==1){
631.                         sprintf(text,"%d", SpO2);
632.                         oled.TextBox((uint8_t *)text,40,25,20,18);
633.                     }else{
634.                        sprintf(text,"");
635.                         oled.TextBox((uint8_t *)text,40,25,20,18);
636.                     }
637.                     if (validHeartRate==1){
638.                         if (first == 0){
639.                             memset(&heartrateArr, heartrate, sizeof(heartrateAr
    r));
640.                             first = 1;
641.                         }
642.                         else
643.                             memmove(&heartrateArr,&heartrateArr[1],sizeof(heart
    rateArr[0])*5);
644.                         heartrateArr[5] = heartrate;
645.                         heartrate = mean(heartrateArr,6);
```

```
646.                         sprintf(text,"%d",heartrate);
647.                         oled.TextBox((uint8_t *)text,35,5,20,18);
648.                     }else{
649.                         sprintf(text,"");
650.                         oled.TextBox((uint8_t *)text,35,5,20,18);
651.                     }
652.
653.                     if (bloodPresureValid==1){
654.                         if (first == 0){
655.                             memset(&bloodPresArr, bloodPresure, sizeof(bloodPre
    sArr));
656.                             first = 1;
657.                         }
658.                         else
659.                             memmove(&bloodPresArr,&bloodPresArr[1],sizeof(blood
    PresArr[0])*5);
660.                         bloodPresArr[5] = bloodPresure;
661.                         bloodPresure = mean(bloodPresArr,6);
662.                         sprintf(text,"%d",bloodPresure);
663.                         oled.TextBox((uint8_t *)text,35,45,20,18);
664.                     }else{
665.                         sprintf(text,"");
666.                         oled.TextBox((uint8_t *)text,35,45,20,18);
667.                     }
668.                 }
669.                 ThisThread::sleep_for(50);
670.             }
671.         }
672.
673.
674.         // the loop function runs over and over again until power down or reset

675.         void ecgTask()
676.         {
677.             //Set ACG configuration
678.             configureEcg();
679.
680.             while (1){
681.                 uint16_t i = 0;
682.                 char final_string[20];
683.                 char time_string[20];
684.
685.                 while (DRDY) {} // wait_ms for ADS1194 device to prepare output
     data.
686.                 ecg2_hal_cs(0);
687.                 wait_us(10);
688.                 for (i = 0; i < num_bytes_sample; i++)
689.                     ecg_data_sample[i] = vspiCommand(0);// read ADS1194 output
    data, one sample
690.
691.                 time_value += 8.0;      // increment time value
692.                 // calculate input voltage
693.                 // voltage LA RA
694.                 channel1_voltage = calculate_ecg_channel( ecg_data_sample, 3, r
    efV, channel_gain, channel1_voltage_offset );
695.                 // voltage LL RA - channel 2 is usually used for simple ECG
696.                 channel2_voltage = calculate_ecg_channel( ecg_data_sample, 5, r
    efV, channel_gain, channel2_voltage_offset );
697.                 pc.printf("%f\n",channel2_voltage);
698.                 sprintf(final_string, "%.2f", channel2_voltage); // convert val
    ues to string and send to MikroPlot
699.                 strcat(final_string, ",");
700.                 sprintf(time_string, "%.2f", time_value);
701.                 strcat(final_string, time_string);
702.                 //pc.printf("%s\n\r",final_string);
```

```
703.
704.                 // voltage LL LA
705.                 channel3_voltage = calculate_ecg_channel( ecg_data_sample, 7, r
    efV, channel_gain, channel3_voltage_offset );
706.                 // voltage from temperature sensor
707.                 channel4_voltage = calculate_ecg_channel( ecg_data_sample, 9, r
    efV, channel_gain, channel4_voltage_offset );
708.
709.                 ThisThread::sleep_for(50);
710.             }
711.         }
```

References

[1] G. Savarese and L. H. Lund, "Global Public Health Burden of Heart Failure," (in eng), *Card Fail Rev,* vol. 3, no. 1, pp. 7-11, Apr 2017, doi: 10.15420/cfr.2016:25:2.

[2] S. R. Toukhsati, A. Driscoll, and D. L. Hare, "Patient Self-management in Chronic Heart Failure - Establishing Concordance Between Guidelines and Practice," (in eng), *Card Fail Rev,* vol. 1, no. 2, pp. 128-131, Oct 2015, doi: 10.15420/cfr.2015.1.2.128.

[3] J. Fergenbaum, S. Bermingham, M. Krahn, D. Alter, and C. Demers, "Care in the Home for the Management of Chronic Heart Failure: Systematic Review and Cost-Effectiveness Analysis," (in eng), *The Journal of cardiovascular nursing,* vol. 30, no. 4 Suppl 1, pp. S44-51, Jul-Aug 2015, doi: 10.1097/jcn.0000000000000235.

[4] C. Eurlings, J. J. Boyne, R. A. de Boer, and H. P. Brunner-La Rocca, "Telemedicine in heart failure-more than nice to have?," (in eng), *Neth Heart J,* vol. 27, no. 1, pp. 5-15, Jan 2019, doi: 10.1007/s12471-018-1202-5.

[5] M. H. Yacoub and C. McLeod, "The expanding role of implantable devices to monitor heart failure and pulmonary hypertension," *Nature Reviews Cardiology,* vol. 15, no. 12, pp. 770-779, Dec 2018, doi: 10.1038/s41569-018-0103-z.

[6] J. S. Kim, S. Y. Hwang, J. L. Shim, and M. H. Jeong, "Cognitive Function and Self-Care in Patients with Chronic Heart Failure," (in eng), *Korean Circ J,* vol. 45, no. 4, pp. 310-6, Jul 2015, doi: 10.4070/kcj.2015.45.4.310.

[7] A. While and F. Kiek, "Chronic heart failure: promoting quality of life," (in eng), *British journal of community nursing,* vol. 14, no. 2, pp. 54-9, Feb 2009, doi: 10.12968/bjcn.2009.14.2.38760.

[8] E. Tanai and S. Frantz, "Pathophysiology of Heart Failure," (in eng), *Comprehensive Physiology,* vol. 6, no. 1, pp. 187-214, Dec 2015, doi: 10.1002/cphy.c140055.

[9] C. Fonseca, D. Bras, I. Araujo, and F. Ceia, "Heart failure in numbers: Estimates for the 21st century in Portugal," (in eng por), *Revista portuguesa de cardiologia : orgao oficial da Sociedade Portuguesa de Cardiologia = Portuguese journal of cardiology : an official*

journal of the Portuguese Society of Cardiology, vol. 37, no. 2, pp. 97-104, Feb 2018, doi: 10.1016/j.repc.2017.11.010. Insuficiencia cardiaca em numeros: estimativas para o seculo XXI em Portugal.

[10] W. Lesyuk, C. Kriza, and P. Kolominsky-Rabas, "Cost-of-illness studies in heart failure: a systematic review 2004-2016," (in eng), *BMC cardiovascular disorders,* vol. 18, no. 1, p. 74, May 2018, doi: 10.1186/s12872-018-0815-3.

[11] C. Cook, G. Cole, P. Asaria, R. Jabbour, and D. P. Francis, "The annual global economic burden of heart failure," (in eng), *International journal of cardiology,* vol. 171, no. 3, pp. 368-76, Feb 2014, doi: 10.1016/j.ijcard.2013.12.028.

[12] W. L. Wilkins E, Wickramasinghe K, Bhatnagar P, Leal J, Luengo-Fernandez R, Burns R, Rayner M, Townsend N " European Cardiovascular Disease Statistics 2017," *European Heart Network, Brussels.,* 2017.

[13] C. Fonseca *et al.*, "Pela melhoria do tratamento da insuficiência cardíaca em Portugal – documento de consenso," *Revista Portuguesa de Cardiologia,* vol. 36, no. 1, pp. 1-8, 2017/01/01/ 2017, doi: https://doi.org/10.1016/j.repc.2016.10.006.

[14] M. Genet, L. C. Lee, B. Baillargeon, J. M. Guccione, and E. Kuhl, "Modeling Pathologies of Diastolic and Systolic Heart Failure," (in eng), *Annals of biomedical engineering,* vol. 44, no. 1, pp. 112-27, Jan 2016, doi: 10.1007/s10439-015-1351-2.

[15] M. King, J. Kingery, and B. Casey, "Diagnosis and evaluation of heart failure," (in eng), *American family physician,* vol. 85, no. 12, pp. 1161-8, Jun 2012.

[16] A. Mosterd and A. W. Hoes, "Clinical epidemiology of heart failure," (in eng), *Heart,* vol. 93, no. 9, pp. 1137-46, Sep 2007, doi: 10.1136/hrt.2003.025270.

[17] G. Shaaya, A. Al-Khazaali, and R. Arora, "Heart Rate As a Biomarker in Heart Failure: Role of Heart Rate Lowering Agents," (in eng), *American journal of therapeutics,* vol. 24, no. 5, pp. e532-e539, Sep/Oct 2017, doi: 10.1097/mjt.0000000000000336.

[18] P. Ponikowski *et al.*, "2016 ESC Guidelines for the diagnosis and treatment of acute and chronic heart failure: The Task Force for the diagnosis and treatment of acute and chronic heart failure of the European Society of Cardiology (ESC)Developed with the special contribution of the Heart Failure Association (HFA) of the ESC," *European Heart Journal,* vol. 37, no. 27, pp. 2129-2200, 2016, doi: 10.1093/eurheartj/ehw128.

[19] Y.-H. Jeon, S. G. Kraus, T. Jowsey, and N. J. Glasgow, "The experience of living with chronic heart failure: a narrative review of qualitative studies," *BMC Health Services Research,* vol. 10, no. 1, p. 77, 2010/03/24 2010, doi: 10.1186/1472-6963-10-77.

[20] S. L. Sayers, B. Riegel, S. Pawlowski, J. C. Coyne, and F. F. Samaha, "Social support and self-care of patients with heart failure," (in eng), *Annals of behavioral medicine : a publication of the Society of Behavioral Medicine,* vol. 35, no. 1, pp. 70-9, Feb 2008, doi: 10.1007/s12160-007-9003-x.

[21] M. W. Rich, V. Beckham, C. Wittenberg, C. L. Leven, K. E. Freedland, and R. M. Carney, "A multidisciplinary intervention to prevent the readmission of elderly patients with congestive heart failure," (in eng), *The New England journal of medicine,* vol. 333, no. 18, pp. 1190-5, Nov 2 1995, doi: 10.1056/nejm199511023331806.

[22] G. C. Fonarow *et al.*, "Impact of a comprehensive heart failure management program on hospital readmission and functional status of patients with advanced heart failure," (in eng), *Journal of the American College of Cardiology,* vol. 30, no. 3, pp. 725-32, Sep 1997.

[23] R. J. Miller and J. G. Howlett, "Does heart rate really matter to patients with heart failure?," (in eng), *Current opinion in cardiology,* vol. 32, no. 2, pp. 209-216, Mar 2017, doi: 10.1097/hco.0000000000000368.

[24] E. Natale and A. Marsocci, "Decreasing heart rate in heart failure: pros and cons," (in eng), *Journal of cardiovascular medicine (Hagerstown, Md.),* vol. 19 Suppl 1, pp. e96-e98, Feb 2018, doi: 10.2459/jcm.0000000000000564.

[25] A. H. Association. "Understanding Blood Pressure Readings." https://www.heart.org/en/health-topics/high-blood-pressure/understanding-blood-pressure-readings. Accessed 02/09/2019.

[26] D. Goyal, R. J. Macfadyen, R. D. Watson, and G. Y. H. Lip, "Ambulatory blood pressure monitoring in heart failure: A systematic review," *European Journal of Heart Failure,* Review vol. 7, no. 2, pp. 149-156, 2005, doi: 10.1016/j.ejheart.2004.05.010.

[27] W. L. Miller, "Fluid Volume Overload and Congestion in Heart Failure: Time to Reconsider Pathophysiology and How Volume Is Assessed," (in eng), *Circulation. Heart failure,* vol. 9, no. 8, p. e002922, Aug 2016, doi: 10.1161/circheartfailure.115.002922.

[28] C. M. Yu *et al.*, "Intrathoracic impedance monitoring in patients with heart failure: correlation with fluid status and feasibility of early warning preceding hospitalization," (in eng), *Circulation,* vol. 112, no. 6, pp. 841-8, Aug 9 2005, doi: 10.1161/circulationaha.104.492207.

[29] V. Sharma, A. Singh, B. Kansara, and A. Karlekar, "Comparison of transthoracic electrical bioimpedance cardiac output measurement with thermodilution method in post coronary artery bypass graft patients," (in eng), *Annals of cardiac anaesthesia,* vol. 14, no. 2, pp. 104-10, May-Aug 2011, doi: 10.4103/0971-9784.81564.

[30] S. Lopez, "Pulse Oximeter Fundamentals and Design," Nov 2011.

[31] J. D. Campbell, C. G. Pretty, J. G. Chase, and P. J. Bones, "A Robust Method of Peak Detection in Noisy PPG Signals Using a Structure of IIR Filters," in *2018 14th IEEE/ASME International Conference on Mechatronic and Embedded Systems and Applications (MESA)*, 2-4 July 2018 2018, pp. 1-6, doi: 10.1109/MESA.2018.8449169.

[32] I. Sudano *et al.*, "Auricall®. A new device for a non-invasive, wireless, continuous monitoring of oxygen saturation and heart rate in patients with heart failure," *International journal of cardiology,* Article vol. 129, no. 1, pp. 141-143, 2008, doi: 10.1016/j.ijcard.2007.06.034.

[33] O. Milo-Cotter *et al.*, "Rapid clinical assessment of patients with acute heart failure: first blood pressure and oxygen saturation--is that all we need?," (in eng), *Cardiology,* vol. 114, no. 1, pp. 75-82, 2009, doi: 10.1159/000213051.

[34] H. M. s. H. Watch. "Salt and your health, Part I: The sodium connection." https://www.health.harvard.edu/newsletter_article/salt-and-your-health. Accessed 05/08/2019.

[35] H. N. Haugen, "A study of sweat electrolyte excretion in a patient suffering from congestive heart failure," (in eng), *Scandinavian journal of clinical and laboratory investigation,* vol. 9, no. 2, pp. 116-21, Jan 1957 1957.

[36] S. Maru *et al.*, "Cost-effectiveness of home versus clinic-based management of chronic heart failure: Extended follow-up of a pragmatic, multicentre randomized trial cohort - The WHICH? study (Which Heart Failure Intervention Is Most Cost-Effective & Consumer Friendly in Reducing Hospital Care)," (in eng), *International journal of cardiology,* vol. 201, pp. 368-75, Dec 15 2015, doi: 10.1016/j.ijcard.2015.08.066.

[37] D. Ruthirago, P. Julayanont, P. Tantrachoti, J. Kim, and K. Nugent, "Cardiac Arrhythmias and Abnormal Electrocardiograms After Acute Stroke," (in eng), *Am J Med Sci,* vol. 351, no. 1, pp. 112-8, Jan 2016, doi: 10.1016/j.amjms.2015.10.020.

[38] A. Rosiek and K. Leksowski, "The risk factors and prevention of cardiovascular disease: the importance of electrocardiogram in the diagnosis and treatment of acute coronary syndrome," (in eng), *Ther Clin Risk Manag,* vol. 12, pp. 1223-9, 2016, doi: 10.2147/tcrm.S107849.

[39] L. National Heart, and and Blood Institute. National Institutes of Health. November 17. ""How the Heart Works"." https://www.nhlbi.nih.gov/health-topics/how-heart-works. Accessed 02/09/2019

[40] E. J. d. S. Luz, W. R. Schwartz, G. Cámara-Chávez, and D. Menotti, "ECG-based heartbeat classification for arrhythmia detection: A survey," *Computer Methods and Programs in Biomedicine,* vol. 127, pp. 144-164, 2016/04/01 2016, doi: https://doi.org/10.1016/j.cmpb.2015.12.008.

[41] L. Ganz, "54 - Electrocardiography," in *Goldman's Cecil Medicine (Twenty Fourth Edition)*, L. Goldman and A. I. Schafer Eds. Philadelphia: W.B. Saunders, 2012, pp. 272-278.

[42] F. Shaffer and J. P. Ginsberg, "An Overview of Heart Rate Variability Metrics and Norms," (in eng), *Front Public Health,* vol. 5, p. 258, 2017, doi: 10.3389/fpubh.2017.00258.

[43] G. Goldich, "12-lead ECGs part II: identifying common abnormalities," (in eng), *Nursing,* vol. 44, no. 9, pp. 30-6; quiz 37, Sep 2014, doi: 10.1097/01.NURSE.0000452990.26288.b4.

[44] R. McFee, "Comparison of Heart Vectors Calculated with Different Systems of Leads," *Circulation,* vol. 2, pp. 128-33, 1950, doi: 10.1161/01.CIR.2.1.128.

[45] M. Nitzan, A. Romem, and R. Koppel, "Pulse oximetry: fundamentals and technology update," (in eng), *Med Devices (Auckl),* vol. 7, pp. 231-9, 2014, doi: 10.2147/mder.S47319.

[46] A. J. Deacon and O. W. Pratt, "Measurement of pulse oximetry, capnography and pH," *Anaesthesia & Intensive Care Medicine,* vol. 18, no. 12, pp. 639-643, 2017/12/01, doi: https://doi.org/10.1016/j.mpaic.2017.09.004.

[47] S. Kennedy, "An Introduction to Pulse Oximeters: Equations and Theory," *University of Wisconsin-Madison,* vol. 20, 2015.

[48] A. A. Alian and K. H. Shelley, "Photoplethysmography: Analysis of the Pulse Oximeter Waveform," in *Monitoring Technologies in Acute Care Environments: A Comprehensive Guide to Patient Monitoring Technology*, J. M. Ehrenfeld and M. Cannesson Eds. New York, NY: Springer New York, 2014, pp. 165-178.

[49] A. Aliverti, "Wearable technology: role in respiratory health and disease," (in eng), *Breathe (Sheff),* vol. 13, no. 2, pp. e27-e36, Jun 2017, doi: 10.1183/20734735.008417.

[50] M. Y. Jaffrin, M. Maasrani, A. Le Gourrier, and B. Boudailliez, "Extra- and intracellular volume monitoring by impedance during haemodialysis using Cole-Cole extrapolation," (in eng), *Med Biol Eng Comput,* vol. 35, no. 3, pp. 266-70, May 1997.

[51] S. Dovancescu *et al.*, "Detecting Heart Failure Decompensation by Measuring Transthoracic Bioimpedance in the Outpatient Setting: Rationale and Design of the SENTINEL-HF Study," (in eng), *JMIR Res Protoc,* vol. 4, no. 4, pp. e121-e121, 2015, doi: 10.2196/resprot.4899.

[52] W. H. W. Tang and W. Tong, "Measuring impedance in congestive heart failure: current options and clinical applications," (in eng), *Am Heart J,* vol. 157, no. 3, pp. 402-411, 2009, doi: 10.1016/j.ahj.2008.10.016.

[53] S. Dovancescu *et al.*, "Sensitivity of a wearable bioimpedance monitor to changes in the thoracic fluid content of heart failure patients," in *Computing in Cardiology*, 2013, vol. 40, pp. 927-930. [Online]. Available: https://www.scopus.com/inward/record.uri?eid=2-s2.0-84894164478&partnerID=40&md5=341bddf7039c7c923194c8952811c50b.

[54] T. Schlebusch *et al.*, "On the Road to a Textile Integrated Bioimpedance Early Warning System for Lung Edema," presented at the Proceedings of the 2010 International Conference on Body Sensor Networks, 2010.

[55] D. S. Picone *et al.*, "Accuracy of Cuff-Measured Blood Pressure: Systematic Reviews and Meta-Analyses," (in eng), *Journal of the American College of Cardiology,* vol. 70, no. 5, pp. 572-586, Aug 1 2017, doi: 10.1016/j.jacc.2017.05.064.

[56] W. W. Nichols and M. F. O'Rourke, *In: McDonald's Blood Flow in Arteries: Theoretical, Experimental and Clinical Principles*. 2005.

[57] J. Solà *et al.*, "Noninvasive and Nonocclusive Blood Pressure Estimation Via a Chest Sensor," *IEEE Trans Biomed Eng,* vol. 60, no. 12, pp. 3505-3513, 2013, doi: 10.1109/TBME.2013.2272699.

[58] R. Mukkamala *et al.*, "Toward Ubiquitous Blood Pressure Monitoring via Pulse Transit Time: Theory and Practice," (in eng), *IEEE Trans Biomed Eng,* vol. 62, no. 8, pp. 1879-901, Aug 2015, doi: 10.1109/tbme.2015.2441951.

[59] P. S. Addison, "Slope Transit Time (STT): A Pulse Transit Time Proxy requiring Only a Single Signal Fiducial Point," (in eng), *IEEE Trans Biomed Eng,* vol. 63, no. 11, pp. 2441-2444, Nov 2016, doi: 10.1109/tbme.2016.2528507.

[60] S. M. Daly, "9 - Biophotonics for blood analysis," in *Biophotonics for Medical Applications*, I. Meglinski Ed.: Woodhead Publishing, 2015, pp. 243-299.

[61] S. Emaminejad *et al.*, "Autonomous sweat extraction and analysis applied to cystic fibrosis and glucose monitoring using a fully integrated wearable platform," (in eng), *Proc Natl Acad Sci U S A,* vol. 114, no. 18, pp. 4625-4630, May 2 2017, doi: 10.1073/pnas.1701740114.

[62] G. Hindricks *et al.*, "Implant-based multiparameter telemonitoring of patients with heart failure (IN-TIME): a randomised controlled trial," *The Lancet,* vol. 384, no. 9943, pp. 583-590, 2014, doi: 10.1016/S0140-6736(14)61176-4.

[63] J. Ritzema *et al.*, "Direct left atrial pressure monitoring in ambulatory heart failure patients: initial experience with a new permanent implantable device," (in eng), *Circulation,* vol. 116, no. 25, pp. 2952-9, Dec 18 2007, doi: 10.1161/circulationaha.107.702191.

[64] B. C. Lampert and S. Emani, "Remote hemodynamic monitoring for ambulatory left ventricular assist device patients," (in eng), *J Thorac Dis,* vol. 7, no. 12, pp. 2165-71, Dec 2015, doi: 10.3978/j.issn.2072-1439.2015.10.45.

[65] A. Gheorghe, U. Griffiths, A. Murphy, H. Legido-Quigley, P. Lamptey, and P. Perel, "The economic burden of cardiovascular disease and hypertension in low- and middle-income countries: a systematic review," (in eng), *BMC Public Health,* vol. 18, no. 1, p. 975, 2018, doi: 10.1186/s12889-018-5806-x.

[66] R. P. Katra, N. Chakravarthy, and I. Libbus, "Remote at-home detection and monitoring of functional chronotropic incompetence in heart failure patients," (in eng), *J Cardiovasc Transl Res,* vol. 4, no. 1, pp. 14-20, Feb 2011, doi: 10.1007/s12265-010-9227-1.

[67] M. S. Kohn *et al.*, "Implementation of a Home Monitoring System for Heart Failure Patients: A Feasibility Study," (in eng), *JMIR Res Protoc,* vol. 6, no. 3, p. e46, Mar 20 2017, doi: 10.2196/resprot.5744.

[68] T. Bombardini *et al.*, "Post-exercise contractility, diastolic function, and pressure: operator-independent sensor-based intelligent monitoring for heart failure telemedicine," (in eng), *Cardiovasc Ultrasound,* vol. 7, p. 21, 2009, doi: 10.1186/1476-7120-7-21.

[69] A. Voss *et al.*, "Smelling heart failure from human skin odor with an electronic nose," (in eng), *Conf Proc IEEE Eng Med Biol Soc,* vol. 2012, pp. 4034-7, 2012, doi: 10.1109/embc.2012.6346852.

[70] R. Dias and J. M. d. Silva, "A Flexible Wearable Sensor Network for Bio-Signals and Human Activity Monitoring," in *2014 11th International Conference on Wearable and Implantable Body Sensor Networks Workshops*, 16-19 June 2014 2014, pp. 17-22, doi: 10.1109/BSN.Workshops.2014.20.

[71] I. G. Trindade *et al.*, "Design and Evaluation of Novel Textile Wearable Systems for the Surveillance of Vital Signals," (in eng), *Sensors (Basel),* vol. 16, no. 10, Sep 24 2016, doi: 10.3390/s16101573.

[72] V. Perez-Jover, M. Sala-Gonzalez, M. Guilabert, and J. J. Mira, "Mobile Apps for Increasing Treatment Adherence: Systematic Review," (in eng), *J Med Internet Res,* vol. 21, no. 6, p. e12505, Jun 18 2019, doi: 10.2196/12505.

[73] G. D. Giebel and C. Gissel, "Accuracy of mHealth Devices for Atrial Fibrillation Screening: Systematic Review," (in eng), *JMIR Mhealth Uhealth,* vol. 7, no. 6, p. e13641, Jun 16 2019, doi: 10.2196/13641.

[74] E. S. Kirkendall, Y. Ni, T. Lingren, M. Leonard, E. S. Hall, and K. Melton, "Data Challenges With Real-Time Safety Event Detection And Clinical Decision Support," (in eng), *J Med Internet Res,* vol. 21, no. 5, p. e13047, May 22 2019, doi: 10.2196/13047.

[75] V. Sytems. "Avoid Mistakes When Selecting a Sensor." https://volersystems.com/v-2018/avoid-mistakes-selecting-sensor/ (accessed 20/07/2019.

[76] m. integrated. "MAXREFDES100#: HEALTH SENSOR PLATFORM." https://www.maximintegrated.com/en/design/reference-design-center/system-board/6312.html. Accessed 10/07/2019.

[77] "Hexiwear." https://os.mbed.com/platforms/Hexiwear/. Accessed 26/07/2019.

[78] Bitalino. "What is BITalino? Is it for you?" https://bitalino.com/en/. Accessed 12/07/2019.

[79] MySignals. "MySignals changes the future of medical and eHealth applications." http://www.my-signals.com/#buy-mysignals. Accessed 12/07/2019.

[80] LifeSignals. "Technology and Tools for Your Development Needs." https://lifesignals.com/products-services/. Accessed 17/08/2019.

[81] L. Young, M. Hertzog, and S. Barnason, "Feasibility of Using Accelerometer Measurements to Assess Habitual Physical Activity in Rural Heart Failure Patients," (in eng), *Geriatrics (Basel),* vol. 2, no. 3, Jul 14 2017, doi: 10.3390/geriatrics2030023.

[82] "Hexiwear." https://www.mikroe.com/blog/hexiwear-user-manual. Accessed 22/08/2019.

[83] "ECG 2 CLICK." [Online]. Available: https://www.mikroe.com/ecg-2-click. Accessed 22/08/2019.

[84] "Understanding the SPI Bus with NI LabVIEW." https://www.ni.com/pt-pt/innovations/white-papers/09/understanding-the-spi-bus-with-ni-labview.html. Accessed 28/07/2019.

[85] *Low-Power, 8-Channel, 16-Bit Analog Front-End for Biopotential Measurements*, Texas Instruments. [Online]. Available: http://www.ti.com/lit/ds/symlink/ads1194.pdf

[86] "HEART RATE 4 CLICK." https://www.mikroe.com/heart-rate-4-click. Accessed 05/09/2019.

[87] C. Basics. "BASICS OF THE I2C COMMUNICATION PROTOCOL." http://www.circuitbasics.com/basics-of-the-i2c-communication-protocol/. Accessed 20/08/2019.

[88] a. Mbed. "IoT Device Development." https://www.mbed.com/en/. Accessed 20/08/2019.

[89] *High-Sensitivity Pulse Oximeter and Heart-Rate Sensor for Wearable Health*. [Online]. Available: https://download.mikroe.com/documents/datasheets/max30101.pdf

[90] MBED. "MAX30101_Finger_Heart_Rate_SpO2_Monitor_Driver_Source_Code." https://os.mbed.com/teams/MaximIntegrated/code/MAX30101_Finger_Heart_Rate_SpO2_Monitor_/. Accessed 30/08/2019.

[91] Y. Liang, D. Abbott, N. Howard, K. Lim, R. Ward, and M. Elgendi, "How Effective Is Pulse Arrival Time for Evaluating Blood Pressure? Challenges and Recommendations from a Study Using the MIMIC Database," (in eng), *J Clin Med,* vol. 8, no. 3, Mar 11 2019, doi: 10.3390/jcm8030337.

[92] M. Elgendi *et al.*, "The use of photoplethysmography for assessing hypertension," *Nature Medicine,* vol. 2, 06/26 2019, doi: 10.1038/s41746-019-0136-7.